Titre: Title:	Microstraining Actiflo(R) Settled Waters as a Pretreatment for UF Membranes
Auteur: Author:	Loreto Araya Vicentelo
Date:	2016
Type:	Mémoire ou thèse / Dissertation or Thesis
Référence: Citation:	Araya Vicentelo, L. (2016). Microstraining Actiflo(R) Settled Waters as a Pretreatment for UF Membranes [Mémoire de maîtrise, École Polytechnique de Montréal]. PolyPublie. https://publications.polymtl.ca/2232/

URL de PolyPublie: PolyPublie URL:	https://publications.polymtl.ca/2232/
Directeurs de recherche: Advisors:	Benoit Barbeau
Programme: Program:	Génie civil

UNIVERSITÉ DE MONTRÉAL

MICROSTRAINING ACTIFLO® SETTLED WATERS AS A PRETREATMENT FOR UF MEMBRANES

LORETO ARAYA VICENTELO

DÉPARTEMENT DES GÉNIES CIVIL, GÉOLOGIQUE ET DES MINES

ÉCOLE POLYTECHNIQUE DE MONTRÉAL

MÉMOIRE PRÉSENTÉ EN VUE DE L'OBTENTION

DU DIPLÔME DE MAÎTRISE ÈS SCIENCES APPLIQUÉES

(GÉNIE CIVIL)

AOÛT 2016

UNIVERSITÉ DE MONTRÉAL

ÉCOLE POLYTECHNIQUE DE MONTRÉAL

Ce mémoire intitulé :

MICROSTRAINING ACTIFLO® SETTLED WATERS AS A PRETREATMENT FOR UF MEMBRANES

présenté par : ARAYA VICENTELO Loreto

en vue de l'obtention du diplôme de : Maîtrise ès sciences appliquées

a été dûment accepté par le jury d'examen constitué de :

M. COMEAU Yves, Ph. D., président

M. BARBEAU Benoit, Ph. D., membre et directeur de recherche

M. BÉRARD Jean-François, M.Sc.A., membre

DEDICATION

To my beloved parents and sisters,

For their unconditional love and support…

ACKNOWLEDGEMENTS

Firstly, I would like to express my appreciation to my research director Dr. Benoit Barbeau, for giving me the opportunity of being one of his students and to work on this project. I will always be grateful for his teaching and priceless advices.

I would also like to thank to the professors Michèle Prévost and Yves Comeau, for sharing their knowledge and experience in the lectures.

I would like to thank to the technical staff at CREDEAU laboratory, for their invaluable professional experience and assistance in the analytical methods and experimental setup implementation: Mireille Blais, Yves Fontaine, Julie Philibert, Jacinthe Mailly, Denis Bouchard, and Melanie Bolduc.

My sincere gratitude goes to Mathieu Lapointe, Evelyne Doré, Sara Kazza and Kim Lompe for offering their time and valuable technical advices.

Thanks to the staff of the Chair on Drinking Water Treatment and Department of CGM, for helping me in different ways: Elise Deshommes, Isabelle Papineau, Valentin Pfeiffer, Laura Razafinjanahary, Shokoufeh Nour, Manon Latour.

Thanks to the students and former students of the Department of CGM, for their company and support: Hadi, Sanaz, Émile, Laura, Celso, Patricia, Oscar, Giovanna, Dominic.

Thanks to Veolia engineers, Edith Laflame and Jean-François Bérard, for their technical support regarding microstrainers and the Actiflo process.

This research project would not have been possible without the cooperation and technical support of the staff of the drinking water treatment facilities of Pont-Viau, Saint-Damase, Lévis, and L'Assomption.

This study was financially supported by NSERC Canada and partners of Industrial Chair on Drinking Water Treatment at École Polyechnique de Montréal.

Thanks to the Comisión Nacional de Investigación Científica y Tecnológica (CONICYT, Chile) for the awarded Postgraduate Master fellowship program.

Finally, thanks to my family, for their support at a long distance, and thanks to Jaime for his caring and comprehension during these past two years.

RÉSUMÉ

Les micro-tamis sont recommandés comme préfiltres pour protéger les membranes à basse pression, soit la microfiltration (MF) ou l'ultrafiltration (UF). Cependant, dans le cas d'un système Actiflo®/UF intégré (procédé Opaline®), le micro-tamis installé entre les deux procédés a présenté des limites opérationnelles, comme une fréquence accrue de rétro-lavages en raison du colmatage rapide des micro-tamis ce qui réduit la productivité. À ce jour, la plupart des études sur la combinaison de la coagulation-floculation avec des membranes d'UF ont ciblées la question de l'encrassement des membranes plutôt que le colmatage des micro-tamis. Par conséquent, l'objectif de ce projet était d'identifier les causes du colmatage des micro-tamis alimentés par un processus Actiflo®. Ceci a été réalisé par (i) la caractérisation des eaux décantées de l'Actiflo® de quatre installations d'eau potable de la province de Québec (Pont-Viau, Saint-Damase, Lévis et L'Assomption); (ii) l'identification des mécanismes d'encrassement des micro-tamis en utilisant le modèle Hermia Unifié et (iii) le développement d'un indice de filtrabilité capables de prédire le taux d'encrassement des micro-tamis. En plus, une évaluation de l'efficacité du rétro-lavage des micro-tamis a été réalisée.

La mise en œuvre d'une installation d'essai de filtrabilité à l'aide de micro-tamis en nylon (100-200 µm) et en acier inoxydable T304 (75-152 µm) en mode *dead-end* a été réalisée, pour obtenir des courbes de variation de perte de charge à un débit constant (vitesse d'approche ≈ 0,08 m/s) qui ont été modélisées avec le modèle d'Hermia Unifié. Le rétro-lavage a été réalisée dans les tamis en acier inoxydable à différentes vitesses de rétro-lavages (0,16-0,35 m/s) sous conditions d'oxydation (jusqu'à 100 mg Cl_2/L de chlore à l'aide de NaOCl) et sous conditions alcalines en utilisant du NaOH jusqu'à atteindre un pH de 12,6.

Selon les résultats, l'encrassement des micro-tamis produit par l'eau décantée des Actiflo® peut être représenté avec le modèle Hermia Unifié avec un bon ajustement pour le tamis en nylon ($R^2 >$ 0,95) et en acier inoxydable ($R^2 > 0,97$). Pour le tamis en nylon à 100 µm, le blocage standard des pores était le mécanisme d'encrassement dominant produit par trois des quatre eaux décantées, lequel était causé principalement par des petits flocs non lestés, ce qui signifie que l'obstruction des pores par microsable était négligeable. Pour les tamis en en acier inoxydable entre 75 et 103 µm, le blocage standard des pores était aussi l'encrassement dominant produit par de l'eau décantée de Pont-Viau, causée principalement par des flocs lestés dont le microsable a eu un effet important

dans le colmatage des pores. Pour le tamis en acier inoxydable à 152 μm, le blocage des pores intermédiaire a été le mécanisme d'encrassement, causé principalement par des flocs non lestés. La concentration des solides en suspension (MES) était le meilleur prédicteur du taux d'encrassement (ou coefficient d'encrassement k_v) obtenu à partir de la modélisation. En conclusion, le microsable et le polymère intégrés dans les flocs ont un effet important sur le type de mécanisme d'encrassement des micro-tamis. Pour les micro-tamis à ouvertures inférieures (associées aux valeurs élevées de k_v), les flocs lestés ont une grande importance, tandis qu'à tailles d'ouverture plus élevés (associées aux faibles valeurs de k_v), ce sont les flocs non lestés qui colmatent. D'autre part, le pH, la vitesse de rétro-lavage et la taille d'ouverture du tamis ont un effet significatif sur l'enlèvement des solides après le rétro-lavage, surtout à un pH élevé (pH >11) lequel a produit l'enlèvement des solides la plus élevée (>80%). Le rétro-lavage avec de l'eau fortement chlorée ne présente pas un effet important sur l'enlèvement des solides (jusqu'à 27%).

Enfin, ce projet de recherche fournit de nouvelles connaissances pour comprendre les mécanismes du colmatage d'une eau décantée d'un processus Actiflo® à micro-tamis, qui pourraient être prises en compte dans l'optimisation de l'opération des Actiflo® et la sélection d'un micro-tamis approprié.

ABSTRACT

Microstrainers has been recommended as a pre-filter to protect low-pressure membranes of microfiltration (MF) or ultrafiltration (UF). However, in the case of an integrated Actiflo®/UF system, the microstrainer installed between the two processes has presented operational limitations, such as increased frequency of backwashing due to fast clogging of microstrainers, which may reduce water productivity. To date, most studies on the combination of coagulation-flocculation with UF membranes have focused on membrane fouling rather than microstrainer clogging. Therefore, the objective of this project was to identify the causes of microstrainers clogging fed by an Actiflo® process. This was carried out by the characterization of the settled waters from Actiflo® of four drinking water treatment facilities of the province of Québec (Pont-Viau, Saint-Damase, Lévis, and L'Assomption); identifying the fouling mechanisms of microstrainers using the Unified Hermia model; and finding water characteristics and a filterability index able to predict the fouling rate on microstrainers. In addition, an evaluation of the backwash efficiency of microstrainers was performed.

The implementation of a filterability test setup using small strainers made of nylon (100-200 μm) and stainless steel T304 (75-152 μm) in dead-end mode was carried out, to obtain head loss variation curves at a constant flow rate (approach velocity ≈ 0.08 m/s) that were fitted to the Unified Hermia model. The backwashing was performed in the stainless steel strainers at different backwash velocities (0.16-0.35 m/s) for oxidizing conditions (up to 100 ppm of chlorine using NaOCl) and alkaline conditions using NaOH to reach up to pH 12.6.

According to the results, the fouling at microstrainers produced by the settled water of Actiflo® can be represented with the Unified Hermia model with a good fit for nylon ($R^2 > 0.95$) and stainless steel ($R^2 > 0.97$) strainers. For the 100 μm nylon strainer, the standard pore blocking was the dominant fouling mechanism produced by three out of four settled waters, caused mainly by small un-ballasted flocs, which means that pore clogging by microsand was negligible. For 75 and 103 μm SS strainers, the standard pore blocking was also the dominant fouling produced by Pont-Viau settled water, caused mainly by ballasted flocs, where microsand has an important effect in pore clogging. For the 152 μm SS strainer, was the intermediate pore blocking, caused mainly by un-ballasted flocs agglomeration. The total suspended solids concentration was the best predictor of the fouling coefficient (k_v) obtained from modeling. In conclusion, both microsand and polymer,

integrated into the flocs, have an important effect on the type of fouling mechanism at microstrainers. The fouling coefficient is sensitive to the strainer opening size, which means finer opening sizes are associated with high k_v values (mainly caused by small ballasted flocs), while larger opening sizes are associated with low k_v values (mainly caused by un-ballasted flocs). On the other hand, the pH, backwash velocity and strainer opening size have a significant effect on solids removal after backwashing. Especially pH under strong alkaline conditions (pH >11) which yielded the highest solids removal (>80%). The backwashing under oxidizing conditions did not present a significant effect on solids removal (up to 27%).

Finally, this research project provides new knowledge to understand the fouling mechanisms of a settled water from the Actiflo® process at microstrainers, which might be considered in the optimization of the Actiflo® operation and the selection of a proper microstrainer.

TABLE OF CONTENTS

LIST OF TABLES

LIST OF FIGURES

LIST OF SYMBOLS AND ABBREVIATIONS

APAM	Anionic polyacrylamide
β	Open area of strainers
BW	Backwashing
CPAM	Cationic polyacrylamide
CW	Clarified water
ΔP	Head loss or differential pressure
DADMAC	Diallyldimethylammonium chloride
DOC	Dissolved organic carbon
DW	Demineralized water
FTIR	Fourier Transform Infrared spectroscopy
FW	Flocculated water
k_v	Fouling coefficient
MDDELCC	Ministère du Développement durable, de l'Environnement et de la Lutte contre les changements climatiques
MF	Microfiltration
MW	Molecular weight
NOM	Natural organic matter
PAM	Polyacrylamide
PDADMAC	Poly(diallyldimethylammonium chloride)
PVDF	Polyvinylidene fluoride
Re_d	Reynolds number based on wire diameter
SCV	Streaming current value

SS	Stainless steel
TOC	Total organic carbon
TSS	Total suspended solids
UF	Ultrafiltration
UV	Ultraviolet
V_s	Cumulative volume filtered per unit surface area

LIST OF APPENDICES

CHAPTER 1 INTRODUCTION

1.1 Background

The interest in using low-pressure membrane processes as an alternative filtration method to replace granular media filters, i.e. sand or sand-anthracite filters, has been increased in drinking water treatment plants, to improve the barrier against colloids, suspended solid, and pathogens, and also to continuously produce good quality water with low energy consumption (Brehant, Bonnelye, & Perez, 2002; Lee, 2000). The low-pressure membranes such as microfiltration (MF) or ultrafiltration (UF) require a pretreatment of the feed water by using microstrainers, in order to remove larger particles able to accelerate membrane fouling and/or plug fiber flow channels. The opening sizes of microstrainers recommended by UF manufacturers ranged between 25 and 1000 μm (MDDELCC, 2015b).

The use of UF membranes downstream of a ballasted flocculation/clarification process (Actiflo®) has been commercialized by Veolia Water Technologies. One operational challenge faced with this application is the excessive clogging of microstrainers possibly due to the export of microsand and/or the residual polymer in settled water. Fast clogging of microstrainers generates repeated sequences of backwash that may reduce water productivity. To date, most studies on the combination of coagulation-flocculation with UF membranes have focused on membrane fouling rather than microstrainer clogging. In this project, the study of the phenomenon of microstrainers clogging as they are fed by Actiflo® settled waters was proposed.

1.2 Objectives

1.2.1 General objective

The purpose of this project is identify the causes of microstrainers clogging fed by an Actiflo® process. In order to accomplish this main goal, the following specific objectives were proposed.

1.2.2 Specific objectives

1. Characterize clarified and flocculated waters collected from four full-scale Actiflo® processes;
2. Identify the clogging mechanisms of microstrainers using the Unified Hermia models;
3. Predict the fouling rate using water characteristics and a filterability index;
4. Evaluate the backwash efficiency of microstrainers.

1.2.3 Research hypothesis

The objectives mentioned above led to verify the following research hypothesis:

- The pore clogging behavior on microstrainers downstream Actiflo® process is represented by the Unified Hermia model.
- The clogging on microstrainers is caused mainly by the residual polymer rather than microsand export.
- The backwash performance of microstrainers is enhanced by alkaline rather than oxidizing conditions.

1.3 Structure of the thesis

Chapter 1 presents a brief introduction and objectives of this research project. Chapter 2 presents a literature review about the Actiflo® process and its application with UF membranes, the action of polymer in water treatment, the prefiltration with microstrainers, and the filtration fouling mechanisms. Chapter 3 explains the methodology used to carry out the specific objectives. Chapter 4 presents the results obtained and discussion. Finally, Chapter 5 presents the conclusions of this thesis.

CHAPTER 2 LITERATURE REVIEW

2.1 Ballasted flocculation/clarification: Actiflo®

The ballasted flocculation/clarification process is commercialized under the name Actiflo® by Veolia Water Technologies. In the following sections, a description of the Actiflo® process and its application in combination with UF membranes will be presented.

2.1.1 Presentation of the technology

Actiflo® is a water treatment technology, which includes in one compact unit the coagulation, flocculation, maturation, and settling steps (Figure 2.1). In the coagulation tank, the addition of coagulant destabilizes the suspended solids and colloidal matter in the influent stream. The water then flows into the injection (or pre-flocculation) tank were polymer and microsand (used as ballast agent) are added to initiate the flocs formation. Next, the water flows through the maturation tank, where a relatively gentle mixing provides ideal conditions for bridging between the microsand, the polymer and the destabilized particles, producing denser flocs than conventional precipitation systems, which increases its settling velocity in the inclined lamella settling tank. The clarified water passes lamellas and is collected into a series of weirs leaving the unit to a downstream filtration treatment. The settled microsand-sludge floc is pumped from the bottom of the settler to a hydrocyclone where the microsand is separated from the flocs and reinjected into the Actiflo® for reuse (Blumenschein, Latker, & Banerjee, 2006; Plum et al., 1998). Typically, 80% of the recycle flow is wasted (sludge) and 20% is pumped back into the injection tank with the microsand (ECO:LOGIC, 2009). Nowadays, the Actiflo® technology is considered validated at full-scale in the province of Québec according to the *Guide de conception des installation de production d'eau potable* (MDDELCC, 2015a).

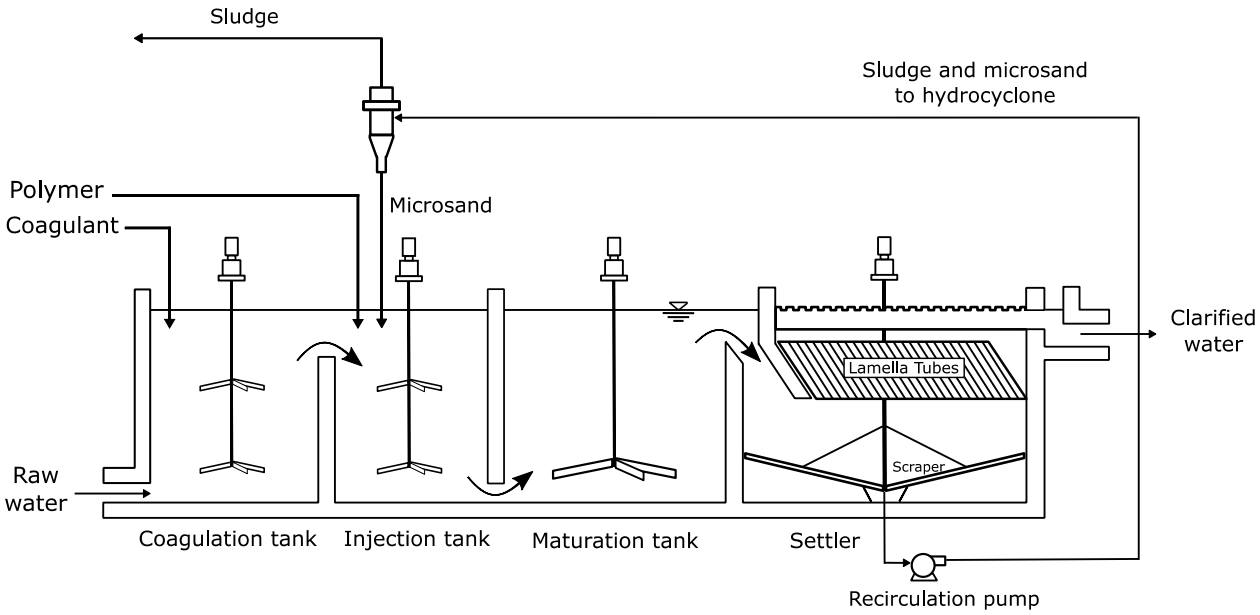

Figure 2.1: Actiflo® process (adapted from Jeschke and Hansen (1999))

2.1.2 Main operational parameters for the Actiflo®

The main control parameters to be considered in the operation of an Actiflo® include the coagulant type and dose, polymer type and dose (anionic, cationic or non-ionic), concentration of microsand in the maturation tank, the microsand diameter and the upflow velocity in the settling step. The Actiflo® settling process can operate with an upflow velocity ranged between 40 to 85 m/h for drinking water applications (Veolia Water Technologies, 2015).

Among the most common coagulants are aluminium sulfate (alum), ferric chloride, ferric sulphate, polyaluminium silicate sulfate (PASS) and polyaluminium chloride (PACl) (Blumenschein et al., 2006; MDDELCC, 2015a). The optimal coagulant dosage will depend of the quality of the water to be treated, e.g., pH, alkalinity, total suspended solids, etc. (R. Desjardins, 1997; MDDELCC, 2015a). In the case of organic polymers used as coagulant in drinking water treatment, typical doses are 1 – 10 mg/L (Bolto & Gregory, 2007) but they are not used in the Actiflo®. Instead, the process uses organic polymers with medium and high molecular weight (typically polyacrylamide or PAM) for improved flocculation. The activated silica can also be used as coagulant aid or flocculant (MDDELCC, 2015a) in the Actiflo® but is typically dosed in combination with PAM. For drinking water treatment, typical doses for organic polymers used as coagulant aids are 0.1 – 0.2 mg/L (Bolto & Gregory, 2007). Nevertheless, the polymer dosage, which is typically slightly higher in

Actiflo® (about 0.3 mg/L), and type will have an important impact on turbidity removal (Blumenschein et al., 2006).

The typical microsand concentration in the maturation tank ranged between 2 to 5 g/L (C. Desjardins et al., 2002; Jeschke & Hansen, 1999). Additionally, it is important to consider that the turbidity of the settled water would increase slightly with increasing concentrations of microsand due to the inability of the floc to hold greater amounts of the ballasting agent, this suggests to find an optimal dose of microsand for each mix of coagulant, polymer dose and source water (Young & Edwards, 2003). On the other hand, the typical effective diameter (d_{10}) of the microsand can range between 50 to 150 μm with a specific gravity of 2.65 (Blumenschein et al., 2006; MDDELCC, 2009). According to Young and Edwards (2003), there are some effects at different sizes of microsand, a significant amount of a larger-size microsand (210 – 300 μm) settled rapidly without being incorporated to the floc. Recently, Lapointe and Barbeau (2016) have shown that the optimal microsand size depends on the final flocs size: large flocs can integrate larger sand grains. Veolia commercializes two microsand sizes to reflect on this observation. The larger media is typically used in wastewater applications while the smaller one is proposed for drinking water applications where the lower coagulant dosages and lower initial suspended solid concentrations lead to small floc sizes (Lapointe & Barbeau, 2016).

2.1.3 UF membranes applications with Actiflo®

It has been reported that some facilities have installed membrane filtration (UF or MF) downstream of the Actiflo® process (Layson, 2010; Lefrançois, 2015). Under such scenario, a microstrainer is installed after settling, prior to the membranes. The microstrainer opening size will vary depending on the membrane technologies. Due to the concerns related to the export of microsand from the Actiflo®, some facilities include microstrainers with low opening sizes (75 – 200 μm) and have subsequently experienced rapid fouling of the microstrainers. In addition, there has also been concern over the impact of residual polymer from the Actiflo® unit on the UF membrane fouling (Lee, 2000). In this study, the use of an anionic polymer at lower dosages (~ 0.117 mg/L) was suggested. In other study about an integrated Actiflo®/MF system (Layson, 2010), it was recommended to prevent overdosing of polymer (>0.3 mg/L) since it will result in large amounts of unreacted polymer leaving the Actiflo® and subsequent membrane fouling. Likewise, the excess of polymer will promote the retention of microsand within membranes, increasing their abrasion.

Therefore, the control of microsand carryover and excess of polymer has taken a major importance in an integrated Actiflo®/membrane system, mainly its impact in useful life of membranes.

2.2 Use of polymers in water treatment

According to Kronberg, Holmberg, and Lindman (2014), a polymer is a large molecule built up of smaller chemical units called monomers and it can have a linear, branched, or cross-linked configuration. When the polymer is synthesized with only one type of monomer, it is termed homopolymer. If the polymer is synthesized with more than one type of monomer, it is termed copolymer. Moreover, the polymers that carry a high net charge are sometimes called polyelectrolytes.

The polymers commonly used in drinking water treatment plants are characterised by their ionic nature: cationic, anionic, and non-ionic. According to their use in coagulation or flocculation, there are other important parameters to be considered in the selection of polymers such as the molecular weight (MW) and charge density (Bolto & Gregory, 2007). Regarding their MW values, can be classified as low ($<10^5$), medium (10^5 - 10^6), and high ($>10^6$). The charge density can be expressed as a percentage of ionic groups relative to all the groups in the polymer (mol%) or as milliequivalents per gram (meq/g). It can be classified as low (ca. 10 mol%), medium (ca. 25 mol%), or high (50 - 100 mol%).

The following sections will focus on cationic and anionic polymers, their adsorption on surfaces and their residual occurrence in water after settling and the resulting impacts on downstream filtration processes.

2.2.1 Cationic and anionic polymers

Cationic and anionic polymers have been generally used in Actiflo® process (Blumenschein et al., 2006; Lee, 2000). The characteristics of both types of polymer are explained below.

2.2.1.1 Cationic polymers

Usually, cationic polymers contain quaternary ammonium groups that have a formal positive charge irrespective of pH, which means that are strong polyelectrolytes (Bolto & Gregory, 2007). Among these polymers, cationic polyacrylamide (CPAM) is widely used in water treatment. It can be used as coagulant (if it has a high charge density) or coagulant aid (if it has a low charge density

and high MW). It can be prepared by copolymerization of acrylamide ($CH_2CHCONH_2$) with a cationic monomer, such as diallyldimethylammonium chloride (DADMAC) (Gregory & Barany, 2011). The molecular structure of CPAM is represented in Figure 2.2. The cationic content in the CPAMs can range between 10 to 100 mol%. Moreover, the hydrolysis of ester groups (RCOOR') and consequent loss of cationic charge of CPAMs has been found to be charge density and pH dependent, thus hydrolysis of CPAMs is promoted under more alkaline conditions (Bolto & Gregory, 2007).

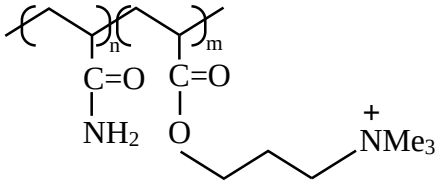

Figure 2.2: Cationic polyacrylamide (adapted from Bolto and Gregory (2007))

Among the natural cationic polymers, the most prominent is chitosan, which has a medium MW and charge density that is pH dependent (e.g., it is slightly charge (17%) at neutral pH levels). On the other hand, starch has a medium MW and the charge density can be low or medium (Bolto & Gregory, 2007).

2.2.1.2 Anionic polymers

Generally, anionic and non-ionic polymers are used in flocculation. The anionic polymers with high MW (10^6 - 10^{12}) allow to start floc formation and also contribute to their growth (Baudin & Fabre, 2006). The most commonly used anionic polymers contain weakly acidic carboxylic acid groups (RCOOH), thus the charge density depends on pH (Bolto & Gregory, 2007). Some anionic polymers are anionic polyacrylamide (APAM)[1], polyacrylic acid (PAA), polyvinyl sulfate, natural biopolymers, etc.

According to Bolto and Gregory (2007), APAM can be prepared either by copolymerisation of acrylamide and acrylic acid or its salts, or by polymerisation of acrylamide (PAM) followed by

[1] APAM is also named as partially hydrolyzed polyacrylamide (HPAM).

partial hydrolysis of amide groups (−$CONH_2$). The charge density of APAM ranged from 10 to 100 mol%. The molecular structure of APAM is presented in Figure 2.3.

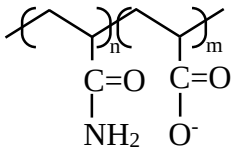

Figure 2.3: Anionic polyacrylamide (adapted from Bolto and Gregory (2007))

APAM and PAM degradation through hydrolysis of its amide groups has been studied (Ma, Shuler, Aften, & Tang, 2015). This hydrolysis can occur under all pH conditions. Both basic and acidic conditions produce a faster hydrolysis than neutral conditions. The reactions of the three mechanisms mentioned before are shown below.

At neutral conditions: $$R\text{–}CONH_2 + H_2O \rightarrow R\text{–}COOH + NH_3 \quad (1)$$

At strong basic conditions: $$R\text{–}CONH_2 + OH^- \rightarrow R\text{–}COO^- + NH_3 \quad (2)$$

At acidic conditions: $$R\text{–}CONH_2 + H_3O^+ \rightarrow R\text{–}COOH + NH_4^+ \quad (3)$$

Ma et al. (2015) also indicate that divalent cations (e.g. Ca^{2+} or Mg^{2+}) at higher concentrations not only can form complexes with the carboxylic groups (−COO^-) on APAM, but also they can catalyze the amide hydrolysis increasing the degree of APAM hydrolysis.

2.2.2 Residual polymer in water and its impact on downstream processes

Firstly, it is important to mention the polymer toxicity in drinking water treatment. In the case of anionic and non-ionic polymers are considered, generally, to have low aquatic toxicity. However, cationic organic polymers are considered to be more toxic to aquatic organisms and, therefore, some countries have restricted their use in drinking water treatment such as Germany and France, while in Japan and Switzerland their use is not allowed (Bolto & Gregory, 2007).

According to the World Health Organization (WHO, 2011), some polymers residues or monomers may escape in finished drinking water, which can pose a potential hazard to human health. This is especially the case for the residual acrylamide monomer of PAMs, which is considered as

"probably carcinogenic to humans". The monomer content is generally 0.05% of the polymer dosage added in water. Considering that in drinking water treatment, the maximum authorized dose of polymer is typically 1 mg/L (it varies from one polymer to another), this suggests a maximum theoretical acrylamide monomer concentration of 0.5 µg/L. Practical concentrations of the residual monomer of the anionic and non-ionic PAM may be lower by a factor of 2 or 3, since acrylamide concentrations are usually controlled by limiting either the acrylamide content of PAM flocculants or the dose of polymer used. Therefore, it is important to avoid overdosing polymer.

Detection of trace acrylamide monomer in water is challenging. Some of the existing analytical techniques to detect acrylamide are summarized in Table 2.1. Determination methods of residual PDADMAC and Epi/DMA polymers, have also been studied (Majam & Thompson, 2006; Mwangi, Ngila, Ndungu, & Msagati, 2013).

Table 2.1: Analytical techniques to determine acrylamide (WHO, 2011)

Analytical technique	**Detection limit [µg/L]**
Gas chromatography (GC/ECD)	0.032
High-performance liquid chromatography (HPLC)	0.2
HPLC with ultraviolet (UV) detection	10

Polymers and their residual contaminants may also react with chemicals added in downstream water treatment processes such as ozonation and chlorination to form undesirable by-products (Majam & Thompson, 2006). The formation of disinfection by-products has been studied following post-chlorination in the presence of cationic, anionic, and non-ionic polymers (Bolto, 2005). The reaction of chlorine with cationic polymers such as PDADMAC or CPAM, at normal residual polymer concentration, produced in general an insignificant level of trihalomethanes (THM) even though the residual acrylamide monomer of CPAM could theoretically be a major THM precursor. In the case of APAM and PAM reaction with chlorine, they also did not form significance levels of THMs.

The degradation of PAM by advanced oxidation ($O_3/H_2O_2/UV$) has also been studied (Ren, Sun, & Chung, 2006). This study indicates that under increasing ozone dosages, more PAMs were

oxidized, where PAM reacted with the formed hydroxyl free radicals (·OH), producing intermediates or final by-products.

2.2.3 Adsorption of polymers on surfaces

The adsorption affinity of polymer to surfaces can be explained by interactions such as electrostatic attraction, hydrogen bonding, hydrophobic interaction, and ion binding. The electrostatic attraction describes the adsorption of polyelectrolytes on surfaces of opposite charge, which gives a very high adsorption affinity and can produce a flatter adsorbed configuration of the polymer, especially with highly charge polyelectrolytes. In the case of hydrogen bonding, the adsorption of a polymer occurs on surfaces with suitable H-bonding sites (e.g. silanol groups on silica) which, for example, can form bonds with the amide groups ($-CONH_2$) of PAM. On the other hand, the hydrophobic interaction is represented by adsorption of non-polar segments of polymer chains on hydrophobic surfaces. Finally, the adsorption by ion binding is promoted at certain concentration of salts with divalent cations such as calcium (Ca^{2+}) and magnesium (Mg^{2+}) (Gregory & Barany, 2011).

The amount of a polyelectrolyte adsorbed on a given charged surface at equilibrium depends on the charge density of both polymer and the surface, the concentration and solubility of the polymer, the chemical affinity of the polymer to the surface and the ionic strength. Moreover, pH can have influence on the polymer and the surface charge, and also the ionic strength (Solberg & Wågberg, 2003). On the other hand, Kronberg et al. (2014) indicates that high MW polymers are more susceptible to adsorb than low MW polymers, and also that a lower solubility of polymers promotes a higher adsorption on surfaces.

In the case of CPAM adsorption on negatively charged silica surfaces, the adsorption and film thickness of the polymer increases as the ionic strength of the solution increases. Although a non-electrostatic interaction have been found between silica and CPAM (Solberg & Wågberg, 2003). In another study, the adsorbed amount of CPAM on silica seems to be independent of the charge density, although when the charge density reaches 10% the presence of hydrophobic segments seems to reduce the amount adsorbed (Samoshina, Diaz, Becker, Nylander, & Lindman, 2003). In addition, decreasing pH can considerably reduce the adsorption of cationic polymers on silica, because the negative charge of the silica is reduced as well (Gregory & Barany, 2011; Kronberg et al., 2014).

APAM adsorption on negative silica surface has also been studied (Samoshina et al., 2003), in which they found that only a small amount of the polymer was adsorbed. Therefore, adsorption of anionic polymers on negative surfaces may require a certain concentration of divalent metal ions, which can bind quite strongly to carboxylate groups ($-COO^-$) of anionic polymers and act as links between these groups and negative sites on a particle surface. Thus, a higher ionic strength (at a certain optimum value) would enhance flocculation (Bolto & Gregory, 2007; Gregory & Barany, 2011). However, flocculation by APAM can be negatively affected in the presence of multivalent metal ions such as Fe^{3+} due to complexation of the metal with carboxylate groups on the polymer chain, decreasing its charge density (Bolto & Gregory, 2007).

According to Guezennec et al. (2015), by increasing temperature the adsorption of APAM on clay surfaces (e.g. kaolinite) will increase. This effect of temperature has the same result for APAM adsorption on PVDF UF membranes (Yi et al., 2012; Yi et al., 2011). On the other hand, according to Kronberg et al. (2014), it is possible to produce the desorption of a polymer from a surface by three different methods. The first one is to add a second component that has a strong affinity with the surface and thus displaces the polymer from the surface. The second method is by manipulating the driving force for adsorption (e.g. counterions), which it is applied for weakly charged polymers subjected to solutions at higher salt concentrations (or ionic strength). The third method is to alter the solubility of the polymer, by changing the pH or by adding a surfactant that associates with the polymer.

2.3 Prefiltration with microstrainers

According to MDDELCC (2015b), UF membranes technologies require a pre-treatment of the feed water by using microstrainers to protect the hollow fibers from damage or fouling from large particles. The microstrainers are mechanical filters that generally include a woven stainless steel screen, which are able to remove particles as fine as 1 µm. However, microstrainers used ahead of UF/MF systems have opening sizes higher than 200 µm typically. Among the advantage of this process are the operational simplicity, small footprint, low complexity in piping and valving (AMIAD Water Systems, 1998). However, one of the main limitations to its use is its tendency to clog rapidly, which may then requires frequent cleaning (AMIAD Water Systems, 2005).

The following sub-sections will focus on the types of microstrainers available and their design criteria, the backwash applied, and the required specifications of microstrainers intended for MF/UF membrane applications.

2.3.1 Type of microstrainers and design criteria

The type of microstrainers include the single basket strainer, duplex or multi-basket strainer, and self-cleaning strainer. Single basket-type strainers have large filtration areas and provide a greater dirt-holding capacity; however, its cleaning requires shutting down the process flow. The duplex or multi-basket strainers can be used for a continuous operation, allowing one of the elements to be on stand-by for cleaning while the other is on duty, although, they must still be watched to check for the need to swap baskets. On the other hand, self-cleaning strainers are an alternative to duplex or multi-basket strainers where continuous operation is critical in the system or where the processes are automated (Sutherland, 2008). Moreover, there are some self-cleaning strainers that include a candle element, which consists of several candle filters connected in parallel, instead of a basket element (BOLLFILTER Protection Systems, 2015).

Microstrainers can be designed with different types of wire mesh such as the wedge-wire and the weave-wire. The latter can have the plain square weave, plain twilled weave, Dutch weave, twilled Dutch weave, or duplex Dutch weave, among others configurations (AMIAD Water Systems, 2005; BOLLFILTER Protection Systems, 2015; Loff, 2001). The most frequently used material is stainless steel (type 304 or 316).

According to AMIAD Water Systems (1998), the design criteria required for the selection of a suitable microstrainer include data such as type of water source, particle size distribution, total suspended solids, minimum and maximum flow rates, system pressure, and nature of solids (i.e. if they are easily breakable or highly charged to promote re-agglomeration downstream of the strainer).

Furthermore, AMIAD Water Systems (2005) indicates that one of the most important parameter to be considered in a microstrainer design is its effective filtration area. The effective filtration area is the total area exposed to fluid flow and it is useful for the filtration process, it does not include the area of the strainer wires. There is another parameter associated with this definition, which is

the open area. The open area refers to the pore area through which the fluid can pass and it is often expressed as a percentage of the effective filtration area.

2.3.2 Backwashing

The single and multi-basket type strainers need to be off-line of the system to be rinsed. The filter element is removed from the strainer chamber, and then is rinsed with water or cleaning solution in a reverse direction from normal flow (AMIAD Water Systems, 2005).

The cleaning procedure of automatic self-cleaning strainers varies according to the different types and models. For example, cleaning by a high velocity suction stream through nozzles connected to a central tube that rotates while removing the filter cake from the strainer is called "suction scanning" (AMIAD Water Systems, 2005). In the case of self-cleaning strainers with candles elements, the cleaning process consists of axial and cross-flow backwash given that the filter candles are open at both ends (BOLLFILTER Protection Systems, 2015).

The backwashing system of automatic self-cleaning strainers can be triggered by either differential pressure or time control (BOLLFILTER Protection Systems, 2015). The maximum differential pressure required to activate the backwashing is generally 7 psig (AMIAD Water Systems, 2005).

The backwashing types mentioned above are hydraulic procedures. Despite those cleaning procedures, the strainers may not reach its initial cleaning condition. Therefore, it can be necessary to use chemical reagents such as alkaline cleaners containing sodium hydroxide (NaOH) or potassium hydroxide (KOH), which are effective against organics and proteins by solubilizing them; or acidic cleaners (pH 1.5 – 2.8) such as phosphoric acid or citric acid which are specially used against inorganic salt/metal fouling. However, hydrochloric acid (HCl) should be avoided because it is very corrosive, especially with stainless steel components. Chlorine is also recommended but its pH should be alkaline (pH 10-11) to minimize corrosion, and it works by a combination of hydrolysis (due to the high pH) and oxidation of organic compounds (Cheryan, 1998).

2.3.3 Required specifications of MF/UF membranes manufacturers for the selection of microstrainers

According to MDDELCC (2015b), the different MF/UF membranes technologies require an upstream microstrainer with opening sizes ranging between 25 and 1 000 µm as it is summarized in Table 2.2. The opening size of the microstrainer varies depending on the type of membrane filtration system and the feed water quality. Furthermore, hollow fiber MF/UF membranes that operate in an inside-out mode are more susceptible to fiber plugging and thus may require a finer prefiltration ranging between 100 to 300 µm (EPA, 2005). This also corresponds to what has been found in some studies, where 200 µm is the most common microstrainer opening size used upstream UF membranes (Brehant et al., 2002; O'Brien, 2006).

Table 2.2: Required microstrainers opening sizes of MF/UF membranes technologies

MF/UF technology products	Microstrainer opening size [µm]
Pall Microza hollow fiber MF (Pall Canada)	up to 400
UF-H_2O Toray (H_2O Innovation)	25 to 150
Pentair X-Flow SXL-225 (Veolia Water Technologies Canada)	200 to 500
ZeeWeed® 1500 (GE Water & Process Technologies)	up to 500
ZeeWeed® 1000 (GE Water & Process Technologies)	500 to 1 000

2.4 Filtration fouling behavior: Unified Hermia model

The "blocking filtration laws" help to visualize and understand the fouling mechanism or behavior of a particle arriving at the surface of a filter medium (Wakeman & Tarleton, 2005). The original Hermia model, which describes the "blocking filtration laws" for Newtonian and non-Newtonian fluids (Cheng, Lee, & Lai, 2011), is expressed by the following general equation at constant pressure filtration (Huang, Young, & Jacangelo, 2008):

$$\frac{d^2t}{dV^2} = k\left(\frac{dt}{dV}\right)^n \tag{4}$$

Where,

V = cumulative volume filtered [m^3]

t = filtration time [s]

n = dimensionless parameter that is related to fouling mechanisms

k = constant parameter

As was mentioned above, the Hermia model is only limited for constant pressure filtration. Thus, a new model was developed to be applied for a constant flux filtration, which is called Unified Hermia model (Huang et al., 2008). This unified model is expressed below.

$$\frac{dP'}{dV_s} = k_v P^n \tag{5}$$

Where,

P' = normalized differential pressure ($P' = P/P_0$)

P = differential pressure through the filter medium

P_0 = initial differential pressure through the filter medium

V_s = cumulative volume filtered per unit surface area of the filter medium [m^3/m^2]

k_v = fouling coefficient [m^2/m^3]

According to Huang et al. (2008), the equation (5) can be converted into a function of normalized specific flux (J'_s), where $J'_s = 1/P' = P_0/P$, obtaining the equation below. This equation is valid for both constant pressure and constant flux filtration.

$$-\frac{dJ'_s}{dV_s} = k_v J'^{2-n}_s \tag{6}$$

By changing the n value according to different modes of fouling and integrating the equation (6), a set of linear equations of the Unified Hermia model is obtained (Table 2.3). Thus, this model describes four different fouling mechanisms at constant flow rate: complete pore blocking, intermediate pore blocking, standard pore blocking, and cake layer formation. These mechanisms are explained in the following sub-sections. The Unified Hermia model has often been used to

estimate theoretically the filtration fouling on low-pressure membranes (MF/UF) (Chellam & Cogan, 2011; Huang et al., 2008).

Table 2.3: Linear equations based on Unified Hermia model (adapted from Huang et al. (2008))

Fouling mechanism	***n***	**Linear expression**
Cake formation	0	$1/J'_s = 1 + k_v V_s$
Intermediate blocking	1	$\mathrm{Ln}(J'_s) = -k_v V_s$
Standard blocking	3/2	$J'^{0.5}_s = 1 - k_v V_s/2$
Complete blocking	2	$J'_s = 1 - k_v V_s$

2.4.1 Complete pore blocking

The complete pore blocking type of fouling refers to every particle in the suspension that is retained on the filter medium only blocks one pore (Ripperger, Gösele, Alt, & Loewe, 2000). This ideal condition assumes that none of the particles are placed on top of other particles or on the solid surface of the filter medium (Huang et al., 2008), as it is represented in Figure 2.4.

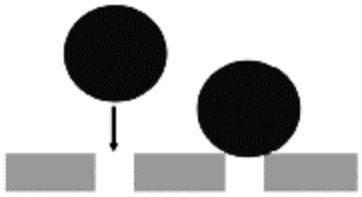

Figure 2.4: Complete pore blocking type of fouling (adapted from Huang et al. (2008))

2.4.2 Intermediate pore blocking

On the contrary of the complete pore blocking, the intermediate pore blocking considers that there is a probability that every particle reaching the surface of the filter medium may not only block the pores, but also may attach on already deposited particles, which means that not every particle will block a pore (Huang et al., 2008; Wakeman & Tarleton, 2005). A diagram of this type of fouling is presented in Figure 2.5.

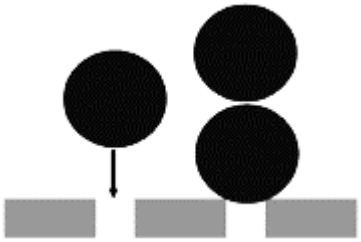

Figure 2.5: Intermediate pore blocking type of fouling (adapted from Huang et al. (2008))

2.4.3 Standard pore blocking

This fouling mechanism of a filter medium, also called "pore constriction", assumes that the pore volume decreases proportionally with the filtrate volume produced due to small particles attached on the walls of the pores. In this case, all pores are assumed to have the same size (Huang et al., 2008; Wakeman & Tarleton, 2005). This entrapment of particles may occur due to diffusional, inertial or electrostatic effects (Wakeman & Tarleton, 2005). This type of fouling is represented in Figure 2.6.

Figure 2.6: Standard pore blocking type of fouling (adapted from Huang et al. (2008))

2.4.4 Cake layer formation

Unlike the three pore blocking types presented above, the cake layer formation (Figure 2.7) does not implicate any changes to the pore structure of the filter medium (Huang et al., 2008). This type of fouling is produced by particles that may be slightly smaller or larger than the pores of the filter medium, and its fouling effect is enhanced by higher concentrations of solids in the feed. If several particles simultaneously reach a pore, there is a probability that they will form a bridge over the pore area. These bridges will support the formation of a cake (Wakeman & Tarleton, 2005).

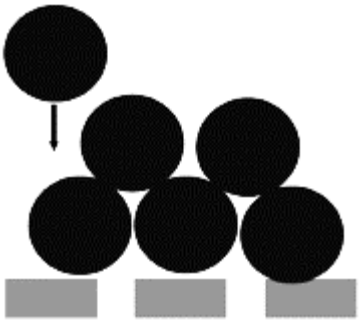

Figure 2.7: Cake layer formation (adapted from Huang et al. (2008))

2.5 Conclusions of the literature review

According to this literature review, in an integrated Actiflo®/membranes system there has been concern about the impact of overdosing polymer and the export of microsand from Actiflo® on downstream UF/MF membranes, where the use of a microstrainer between the two processes has helped to cope with this issue. However, the frequent backwashing on the microstrainers due to its fast clogging it has converted in a new operational concern.

Regarding the study of the pore clogging or fouling behavior at microstrainers by using a filtration model, for example, the Unified Hermia model, to the best of our knowledge, no information has been found. The Unified Hermia model has been generally applied to low-pressure membranes. This lack of information led us to our main research hypothesis: the pore clogging behavior on microstrainers fed with clarified water from Actiflo® can be represented by the Unified Hermia model.

On the other hand, the adsorption affinity of polymers on different type of surfaces led us to other research hypothesis: the residual polymer in settled waters is the main cause of the pore clogging at microstrainers rather than microsand export.

Finally, the faster degradation of polymers (i.e. PAM or APAM) by strong basic conditions, led us to the last research hypothesis: the backwash performance of microstrainers is enhanced by alkaline rather than oxidizing conditions.

CHAPTER 3 MATERIALS AND METHODS

This chapter describe the methodology applied to carry out the objectives of this research project. The methodology involves the characterization of various effluent waters from Actiflo® processes applied in the province of Québec, the development of a filterability test on microstrainers, the estimation of a filterability index based on a 0.45 μm membrane filter, the experimental design of backwashing tests on clogged microstrainers, data analysis, and characterization of clogging on microstrainers.

3.1 Sampling sites and type of water

The sampling sites selected were all drinking water treatment facilities of Québec, which have been using the Actiflo® process: Pont-Viau (Laval), Saint-Damase, Lévis, and L'Assomption. Pont-Viau plant is one of three plants that supplies drinking water in Laval city (Ville de Laval, 2003). The source of raw water for this plant comes from the *Rivière des Prairies*. In the case of Saint-Damase plant, the source of raw water comes from the Yamaska River. Water samples were also obtained from an Actiflo® pilot located in the Lévis plant. Its raw water intake comes from the Saint Lawrence River. L'Assomption plant obtains raw water from the L'Assomption River.

Two types of water from Actiflo® process were characterized: clarified water (CW) and flocculated[2] water (FW). Flocculated water was used in order to produce a lower water quality of the original clarified water for further filterability tests (see section 3.3).

Thus, a filterability test in laboratory was performed to evaluate the fouling potential of the following water qualities:

- Clarified water
- Flocculated water
- 90% CW + 10% FW
- 70% CW + 30% FW

[2] Flocculated water was obtained from the Actiflo® maturation tank.

In addition, the operational conditions of Actiflo® of the four drinking water facilities during the sampling (period between June to November 2015) are described in Table 3.1. The microsand concentration refers to the concentration in the maturation tank. However, in the case of Pont-Viau only the microsand dose is available (1.5 g/m^3). The microsand dose represents the average loss of microsand from the process.

Table 3.1: Actiflo® operational conditions of four drinking water facilities

Plant	**Upflow velocity [m/h]**	**Coagulant dose (Alum) [mg Al/L]**	**Polymer**		**Microsand concentration [g/L]**
			Type	**Dose [mg/L]**	
Pont-Viau	49	48	Hydrex 3511 (anionic)	0.22	N.A.
Saint-Damase	35 - 40	40.5	Magnafloc (anionic)	0.37	5 - 8
Lévis	80	17	LT22S (cationic)	0.20	5 - 6
L'Assomption	10	4.8	C-492 (cationic)	0.21	1.96

3.2 Characterization methods of water samples

The characterization of the water samples comprises the following analytical methods. Turbidity was measured using a calibrated turbidimeter Hach 2100N. pH was determined using pH-meter Accumet Basic AB15. Other analytical methods based on Standard Methods (APHA, AWWA, & WEF, 2012) were used such as total suspended solids (TSS) and volatile suspended solids (VSS), methods 2540D and 2540E, respectively; total and dissolved organic carbon (TOC and DOC), method 5310B; UV absorbance (UV_{254nm}) of organic compounds, method 5910B; and alkalinity measured by potentiometric titration method (2320B). On the other hand, particle concentration and size distribution were determined using Brigthwell DPA4100 SP1 at low magnification (particle sizing range between 2 to 300 μm). Streaming current value (SCV) of the particles was measured using Chemtrac ECA 2100 (sensitivity: low, gain: 1X, and zero offset: 0). Determination of total and soluble aluminum by Inductively Coupled Plasma Atomic Emission Spectroscopy

(ICP-AES, Thermo Scientific iCAP 6300) in conjunction with ultrasonic nebulizer CETAC U5000T+ , using a wavelength of 308.2 nm, with a detection limit of 10 ppb.

Regarding the characterization of residual polymer in clarified water, as was mentioned in the literature review, due to the difficulty to determine acrylamide at very low concentrations and complexity of the existing methods this parameter was not measured. However, the polymer adsorbed on microstrainers was analyzed, the method is explained in section 3.6.

3.3 Filterability tests

Two types of filterability tests were carried out, the first one consist of filterability on microstrainers ranging between 75 to 200 μm, and the second one was applied on a 0.45 μm membrane filter. Both are explained in the following sub-sections.

3.3.1 Filterability on microstrainers

The filterability test on microstrainers was performed on various opening sizes using two materials: nylon (100 and 200 μm) and stainless steel T304 (75, 103, 152 μm). The open area of the SS strainers of 75, 103, and 152 μm are 46%, 37%, and 38%, respectively. Different water qualities (see section 3.1) of four Actiflo® processes (Pont-Viau, Saint-Damase, Lévis, and L'Assomption) were evaluated using different nylon strainers in the laboratory. On the other hand, clarified water from Pont-Viau Actiflo® was selected to test the different opening sizes of the SS strainers, which required a greater volume of water. Thus, tests were performed on site.

The filterability tests (Figure 3.1) at laboratory consist of a dead-end filtration mode. 10 L water sample, homogenously mixed (gradient velocity, $G \approx 100\ s^{-1}$), is pumped at 0.36 ± 0.01 L/min using a peristaltic pump (Masterflex I/P drive with Easy-Load head), to a stainless steel filter holder (diameter = 13 mm) which contains the nylon strainer and below of it a 300 μm SS support. The filtration area is about 0.79 cm^2. During the test, the pressure of the system was registered every 30 seconds. The test was stopped after the filtration of 10 L of sample or when reached a high differential pressure (> 7 psig). Images of the experimental setup can be found in Appendix A.

The filterability tests on site (Pont-Viau) consist in the filtration of clarified waters pumped at 0.37 L/min directly from the Actiflo® (see operational data in Appendix B) using the same experimental setup as above. In this case, SS strainers were used, without a support below them. The filterability

test is stopped when the differential pressure reaches 7 psig, this in order to reproduce real full-scale operational conditions. Then, the clogged strainers were subjected to further backwashing tests.

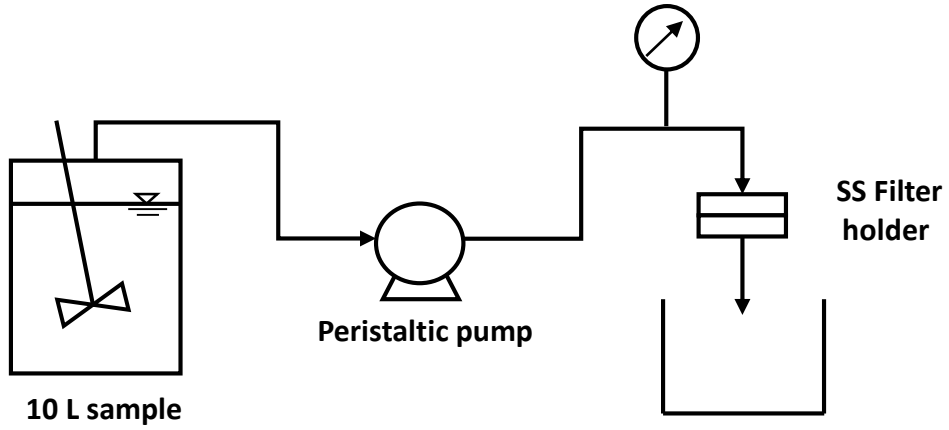

Figure 3.1: Schematic diagram of the filterability test on microstrainers

3.3.2 Filterability on a 0.45 µm membrane filter

The purpose of this filterability test is to obtain a filterability index (FI), which might be able to correlate with the fouling parameter obtained from the filterability on microstrainers (section 3.3.1). The 0.45 µm filterability test is commonly used by VEOLIA as a method to evaluate the fouling propensity of Actiflo® clarified waters for granular media filters. The materials needed for this test are a 0.45 µm polyethersulfone (PES) membrane filter, 47 mm (Supor®-450, Pall), a filter holder with funnel, 1 L side-arm flask, vacuum pressure gauge, and a chronometer. The test consists of registering the filtration time of 200 mL of water sample that passes through a membrane filter (previously wetted with demineralized water (DW)) at a constant vacuum pressure of 495 mmHg (19.5“Hg or 9.6 psig).This is based on the method developed by C. Desjardins et al. (2002). This filterability test was applied to the water sample and a blank using DW, and it was carried out in triplicates. Then, the FI was estimated as follows (Tramfloc, 2014).

$$FI = \frac{Sample\ time}{Blank\ time} \tag{7}$$

3.4 Backwashing tests

Backwashing tests were performed after the filterability tests on SS microstrainers on site (Pont-Viau). The fouling on microstrainers was exposed to oxidizing and alkaline cleaning conditions. For the former, chlorine (as sodium hypochlorite, NaOCl) was selected, and for the latter, sodium hydroxide (NaOH). The respective cleaning solutions were prepared on site by adding the reagents mentioned before into filtered water obtained from the filtration process of Pont-Viau plant. The volume of the cleaning solution was determined by the backwashing flow rate and time used. Backwashing was in reverse direction of normal flow and lasted 5 min (3 min of cleaning solution followed by 2 min of rinse with filtered water).

The backwashing test with chlorine for both 75 and 103 μm SS strainers was performed under the following conditions:

- Backwashing velocities: 0.16 and 0.24 m/s (0.6 and 0.9 L/min, respectively)
- Chlorine concentrations: 0, 10, and 100 ppm Cl_2

On the other hand, the backwashing test with the alkaline solution for 75, 103, and 152 μm SS strainers was performed under the following conditions:

- Backwashing velocities: 0.16, 0.24, and 0.35 m/s (0.6, 0.9, and 1.35 L/min respectively)
- pH: 5.9 (ambient filtered water pH), 11.0, and 12.6

The backwashing efficiency of these tests was estimated by solids removal on SS strainers using the procedure below:

1) Determination of retained solids at 105 °C for 1 h (after filterability test (FT), duplicate)
2) Determination of retained solids at 105 °C for 1 h (after backwashing (BW))
3) Calculation of solids removal:

$$Solids\ removal\ (\%) = \frac{(Retained\ solid\ after\ FT - Retained\ solids\ after\ BW)}{Retained\ solid\ after\ FT} \times 100 \qquad (8)$$

3.5 Data analysis

The normalized differential pressure and the cumulative specific volume of filtrate, obtained during the filterability test, will be used to evaluate the fouling behavior on microstrainers using the linear equations of Unified Hermia model, and thus finding a fouling coefficient (k_v). STATISTICA 12 software was used for modeling the data.

The different factors (such as strainer opening size, BW velocity, Cl_2 concentration, and pH) affecting the backwashing efficiency (or solids removal) of both oxidizing and alkaline conditions were analyzed by a factorial ANOVA (2x2x3 for the first condition and 3x3x3 for the second one) with a statistical significance level $\alpha = 0.05$ (using STATISTICA 12 software). In addition, a main effects ANOVA was carried out to analyze all data, which include both backwashing conditions. This means to analyze the significance difference between pH levels reached by an alkaline solution and by chlorine solution (pH 8.0 and 9.4 for 10 and 100 ppm Cl_2, respectively), as well as verify if there is a significance difference between different strainer opening sizes and BW velocities.

3.6 Characterization of clogging on strainers

Using microscopy images at 10X magnification (OLYMPUS BX51 microscope and camera DP70) of the different strainers after filterability tests, help to visualize and understand the fouling behavior model. In addition, microscopy images were taken after backwashing tests.

The presence of polymer (APAM) adsorbed on stainless steel strainers after filterability and backwashing tests was determined by Fourier Transform Infrared spectroscopy (FTIR) using a Spectrum 65 from Perkin-Elmer. The infrared (IR) spectrums of SS strainers were compared with the IR spectrum of a pure dry commercial APAM (Hydrex 3511). This polymer is used in Pont-Viau.

CHAPTER 4 RESULTS AND DISCUSSION

This chapter comprises the results and discussion according to the objectives proposed for this research project. First, the settled waters under investigation were characterized. In a second section, results of filterability assays will be presented. The third section will report the analysis of the fouling mechanisms.

4.1 Settled water characteristics

The characterization of clarified water (or settled water) from the Actiflo® of Pont-Viau, Saint-Damase, Lévis, and L'Assomption drinking water facilities is summarized in

Table 4.1, for a sampling period spanning from June to November 2015. Regarding pH values, they ranged between 6.8 and 7.6, with the highest value observed in Lévis (fed by the St Lawrence River). The higher turbidity values were observed in Lévis and L'Assomption, meanwhile lower values were observed in Pont-Viau and Saint-Damase, all these turbidity values complies with the target suggested by Kawamura (2000) for a clarifier effluent (< 2 NTU). The streaming current value (SCV) is an indicator of the electric charge of the suspended particles in solution. All of the four clarified waters had a negative charge, especially in Pont-Viau, which implied that full charge neutralization was not achieved in these waters. Total organic carbon (TOC) of all clarified waters indicates a potential for disinfection by-products (DBP) formation, since their values exceed 2 mg C/L (USEPA, 1999). In addition, the organic matter content in clarified water of Saint-Damase suggests that with the coagulation was not optimized as the SUVA[3] value recommended for a filtered water was higher than 2.0 L/mg C·m^{-1} (Kawamura, 2000). It is important to consider the organic matter content since it has been reported that it has an inversely effect on APAM adsorption on negatively charged particle surfaces (Lu, Wu, & Letey, 2002). The VSS to TSS ratio ranged between 16 to 55%, with the highest value observed for Pont-Viau and the lowest in Lévis. This suggests that clarified water from Pont-Viau has the highest organic content, and in the case of Lévis, there is more presence of inorganic compounds, which can be explained due to a higher microsand export caused by a high upflow velocity in the Actiflo® process (80 m/h) at the time of

[3] SUVA is the normalized value of UV_{254nm} by dissolved organic carbon (DOC).

sampling. The TSS to turbidity unit ratio ranged between 1.2 to 4.9 mg/L/NTU for the different clarified waters, with higher ratios observed in Pont-Viau, Saint-Damase, and Lévis. These values are considered high when compared with the ratios of 0.7-2.2 found for low-color raw waters (Letterman & American Water Works Association., 1999). Such result is coherent with the potential presence of microsand in settled waters, which is expected to have more impact on TSS than turbidity due to the high density of sand particles as opposed to natural surface water particles. The minimum value of total residual aluminum was found in clarified water from L'Assomption (0.22 mg/L) and the maximum value was found in Lévis (0.43 mg/L). Total aluminium was mostly composed of particulate aluminum from the microflocs, since dissolved aluminum was always below 50 µg/L for all clarified waters.

Table 4.1: Clarified water characterization of various drinking water facilities with Actiflo®

Parameter	**Unit**	**Clarified water – Actiflo®**			
		Pont-Viau	**St-Damase**	**Lévis**	**L'Assomption**
pH		6.83	7.19	7.57	6.76
Temperature	°C	22	19	21	22
Turbidity	NTU	0.42	0.54	0.88	0.92
Alkalinity	mg $CaCO_3$/L	17	58	70	24
Conductivity	µS/cm	108	288	285	271
SCV		-326	-152	-155	-110
DOC	mg C/L	3.04	3.82	2.47	2.27
TOC	mg C/L	N.A.	3.91	2.55	2.36
$SUVA_{254nm}$	L/mg C·m^{-1}	1.8	2.2	1.6	1.5
TSS	mg/L	2.0	1.8	4.2	1.1
VSS	mg/L	1.1	0.60	0.67	0.55
VSS/TSS	%	55	33	16	50
TSS/Turbidity	mg/L/NTU	4.9	3.4	4.7	1.2
Particles concentration (> 2 µm)	#/mL	1 434	1 561	3 135	2 641
Soluble aluminum	µg/L	13.9	37.5	40.6	11.4
Total aluminum	µg/L	317	250	433	216

Particles concentration (> 2 µm) varied from 1 400 to 3 200 counts/mL and were generally in agreement with turbidity measurements. The particle size distribution of the clarified water of the

four sources ranged between 2 to 110 μm. In clarified waters from Pont-Viau, Saint-Damase, Lévis, and L'Assomption, it was found that 100%, 99.1%, 100%, and 100% of the particles, respectively, were finer than 85 μm. This particle size was selected as reference since it is the standard effective diameter of microsand generally used in Actiflo®. This suggests that only small flocs remained in clarified water after settling. Their size is small compared with the mean size of flocs (310 μm) formed with microsand/PAM during the maturation process (Lapointe & Barbeau, 2016). Considering the pore opening size of the microstrainers investigated in this project (75 to 200 μm), it is anticipated that pore blocking might be a potential fouling mechanism.

Finally, the flocculated waters from Pont-Viau, Saint-Damase, and Lévis had TSS concentrations of 12, 542, and 178 mg TSS/L, respectively (no data is available for L'Assomption). The low TSS concentration in the case of Pont-Viau is due to sampling at the top of the water column in the maturation tank. This characterization is used as reference for some filterability test results in which flocculated waters were used to produce degraded settled waters. Other characteristics of these flocculated waters are presented in Appendix C.

4.2 Filterability test on microstrainers

The clogging of a porous medium usually translates as an increase of the pressure drop or head loss (Hodur, 2008). As it is shown by the curves obtained from the filterability tests (Figures 4.1, 4.3, 4.4, and 4.5), using nylon microstrainers with a pore size of 100 μm, where the Y-axis is represented by the head loss (ΔP) of the filtration system and X-axis is the specific filtered volume (V_s). A 7-psi head loss was set as a reference, according to microstrainers manufacturers, to identify when a strainer is considered clogged and backwashing is activated. Clarified water from Lévis (Figure 4.1) caused the fastest increase in head loss (reaching 7 psi in 17 min), which suggests a fastest clogging on the strainer pores. When compared with a 200 μm strainer (Figure 4.2), there were no variations of pressure during the filterability test for all clarified waters. A constant head loss of 1.5 psi was maintained for about 25 min of filtration, which means that the 200 μm strainers pores have not been clogged enough to reach a 7 psi head loss. We can conclude that the fouling rate is quite sensitive to the microstrainer opening size.

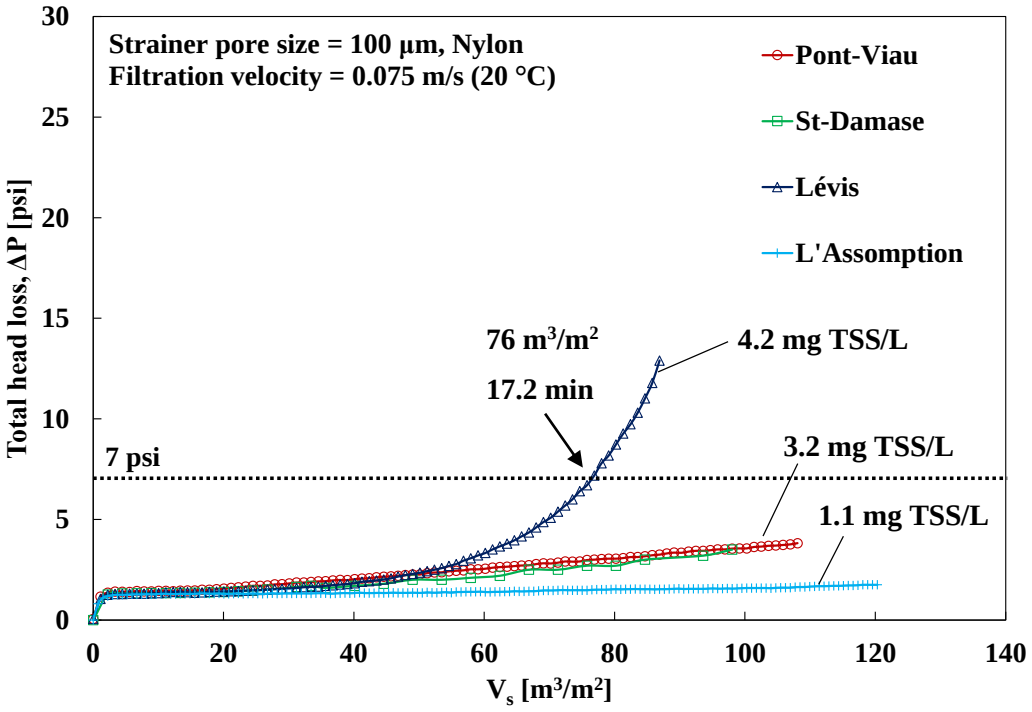

Figure 4.1: Pressure variation during filterability of various clarified waters using a 100 µm nylon strainer

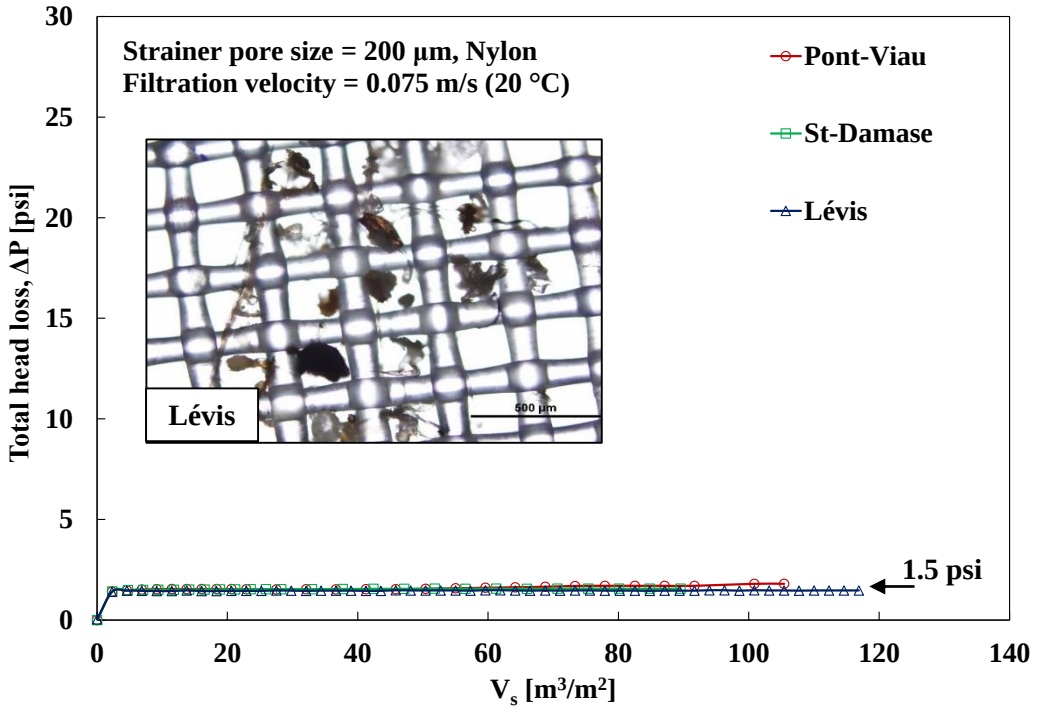

Figure 4.2: Pressure variation during filterability of various clarified waters using a 200 µm nylon strainer. It includes image of 200 µm strainer after filterability of Lévis clarified water

For a lower water quality (achieved by mixing flocculated waters with settled waters), the variation of pressure during filterability using a 100 µm nylon strainer was measured. The pressure variation obtained for a water mixture prepared with 90% clarified water and 10% flocculated water from various Actiflo® is presented in Figure 4.3, while results for mixture prepared with 70% clarified water and 30% flocculated water is shown in Figure 4.4. In addition, 100% flocculated waters were also subjected to a filterability test, using samples from Saint-Damase and Lévis, which both had a higher TSS concentration (Figure 4.5). As expected, the duration time of the filterability test and specific filtered volume (V_s) is reduced when the water quality decreases. It can also be noted in Figure 4.3 and Figure 4.4, that for two waters, the fouling increases exponentially while for Pont-Viau, the increase is linear. Pont-Viau flocculated waters were very low in turbidity (12 NTU as opposed to 178-542 NTUs for Saint-Damase/Lévis) which most likely explains their relative minor impact on fouling.

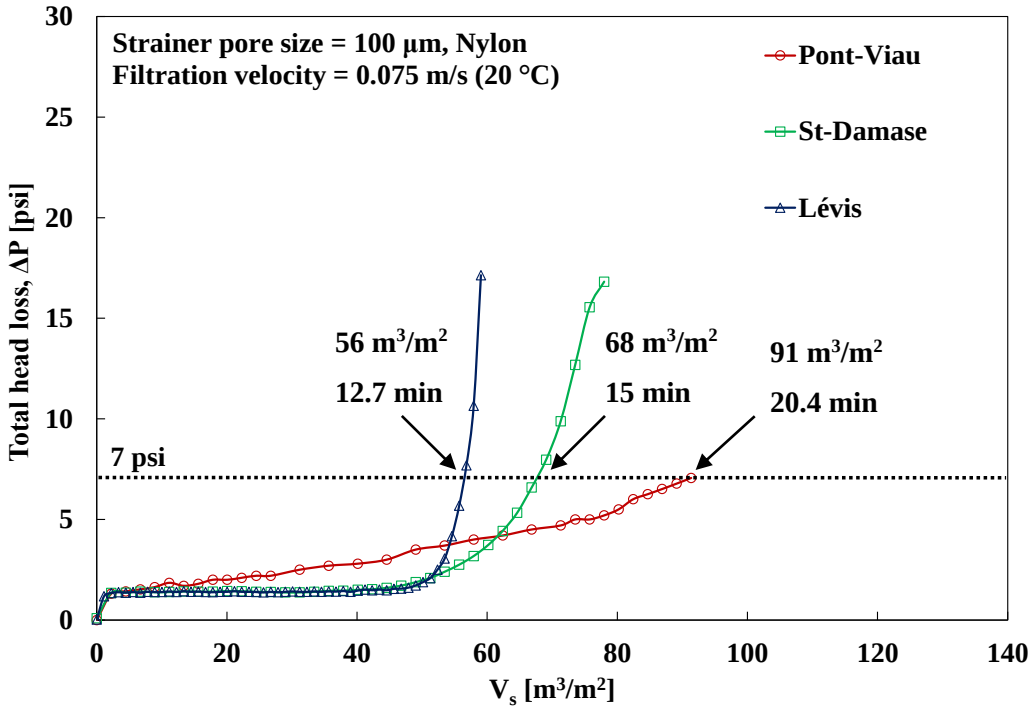

Figure 4.3: Pressure variation during filterability of a mixed water (90% = CW, 10% = FW)

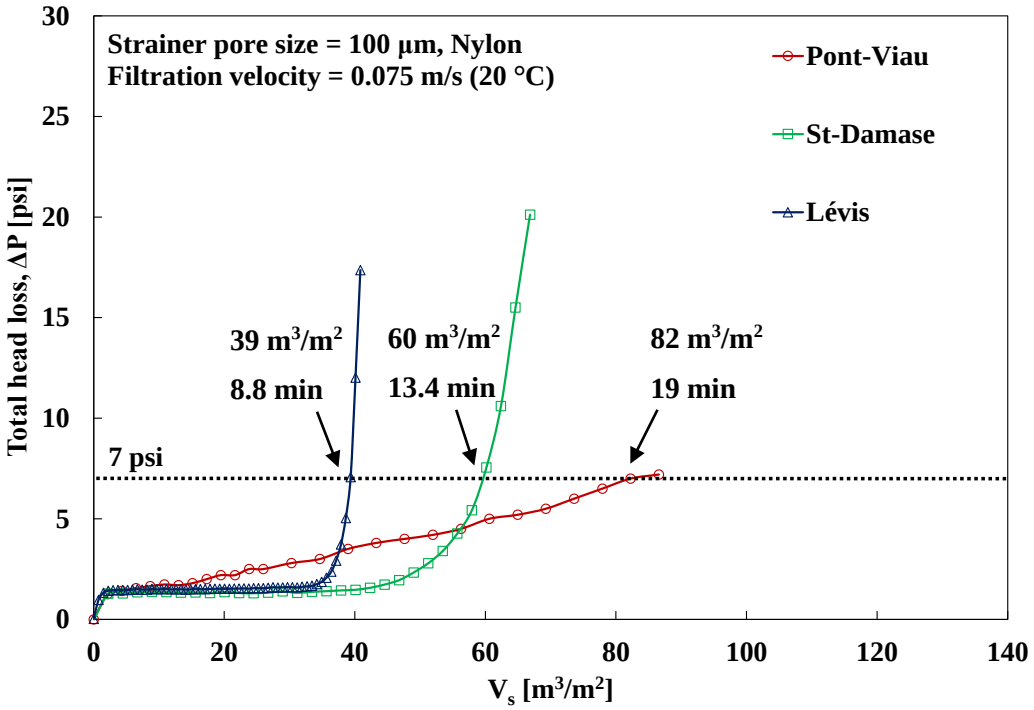

Figure 4.4: Pressure variation during filterability of a mixed water (70% = CW, 30% = FW)

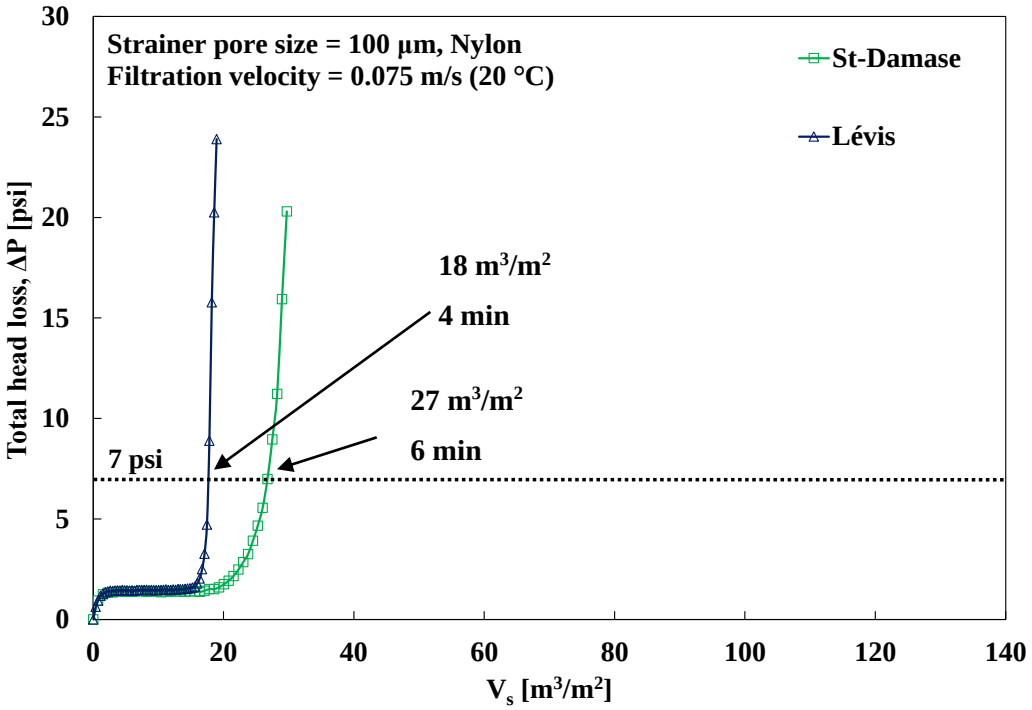

Figure 4.5: Pressure variation during filterability of 100% flocculated waters using 100 µm nylon strainer

Additional filterability assays were performed on site at Pont-Viau plant in order to test stainless steel strainers as opposed to nylon strainers. In addition, three opening sizes were tested: 75, 103 and 152 µm. The filtration pressure curves for these tests are presented in Figure 4.6. The main characteristics of the Actiflo® clarified waters were 3.0 ± 1.5 mg TSS/L, 31 ± 5% VSS/TSS, 0.99 ± 0.43 NTU, pH 6.94 ± 0.01, and 1444 ± 634 particles/mL (see water characteristics used for each SS strainer in Appendix D). The bigger the pore size, the longer is the duration of the filterability test and the higher is the clarified water volume required to achieve a clogged strainer (at 7 psi of head loss). For 75, 103 and 152 µm strainers, the mean values of specific filtered volume and filtration time obtained at 7-psi head loss were 111 ± 15 m^3/m^2 (24 ± 3 min), 203 ± 24 m^3/m^2 (43 ± 5 min), and 487 ± 54 m^3/m^2 (103 ± 11 min), respectively. Once again, the results indicate that the fouling rate is very sensitive to the microstrainer opening size. Figure 4.6 also illustrates fouling rates for several replications tests (about 10x for each strainer). Variability was observed from one replicate to another. The statistical significance of this variability will be further discussed in the

section 4.4.2. Finally, considering that the tests on nylon and SS strainers were not done in parallel, no attempt was made to compare the results.

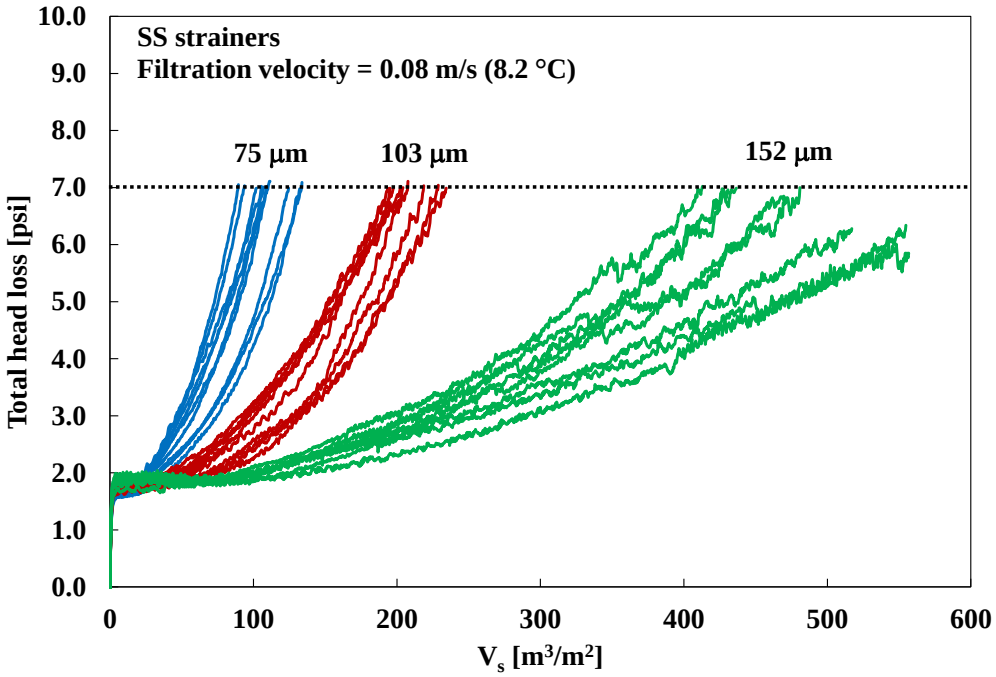

Figure 4.6: Replicates of pressure variation during filterability of clarified water on site (Pont-Viau) using different SS strainer opening sizes. 75 µm (blue), 103 µm (red) and 152 µm (green)

In terms of productivity (in m^3/m^2), the filterability tests (on nylon and SS strainers) can be considered representative of a full-scale microstrainer in operation. For example, a commercial microstrainer (AMIAD 8" EBS 10000) which has similar operational conditions as the tests (initial head loss = 1.4 psi at maximum flow rate = 270 m^3/h) and a filtration area of 1.0 m^2 (AMIAD Water Systems, 2016), it can treat from 45 to 540 m^3/m^2 if it operates from 10 to 120 min. This productivity is similar as the filterability tests, assuming a 7-psi head loss will be reached at those times. Although, there is no specific information available about the productivity of commercial microstrainers based on opening size.

4.3 Impact of water quality on fouling

In this section, the results of the fouling mechanisms on microstrainers were determined by fitting the Unified Hermia model, according to different water qualities. Fitting the Unified Hermia model implies adjusting by nonlinear regression the fouling coefficient (k_v). Once this task was achieved, we attempted to identify water characteristics controlling the fouling coefficient. Finally, the fouling coefficient was correlated with the 0.45 µm filterability index typically used to evaluate the propensity of a settled water to generate head loss on a rapid dual-media granular filter (C. Desjardins et al., 2002) or to evaluate the performance of direct filtration (Tchio, Koudjonou, Desjardins, Prévost, & Barbeau, 2003).

4.3.1 Evaluation of fouling mechanisms

The fouling mechanisms determined by the Unified Hermia model on 100 µm nylon strainer are presented in Table 4.2. For the four clarified waters, the standard pore blocking mechanism was the dominant fouling type, with the exception of complete pore blocking presented in Lévis water. Such result is coherent with the opening sizes of the strainers vs. the particle size distribution characterized in section 4.1, i.e. the particle sizes are lower than the strainer opening sizes which is more favourable to pore blocking as opposed to cake formation (Huang et al., 2008). In some mixed waters and flocculated waters of Saint-Damase and Lévis, the Unified Hermia model did not provide an adequate fit (5 assays out of 12 assays fitted). However, in general the performance of the model was excellent ($R^2 > 0.95$). Regarding the waters mix of 90% CW and 10% FW, a complete pore blocking and intermediate pore blocking mechanisms were determined. For a 70% CW and 30% FW, cake layer formation and complete pore blocking were determined. In the case of 100% flocculated waters, which has a very high concentration of TSS, the possible fouling mechanisms were complete pore blocking and cake layer formation.

Microscopy images of the 100 µm nylon strainers samples clogged with the four different clarified water sources are presented in Figure 4.7. It can be observed more presence of microsand along with the flocs on the microstrainer tested on Lévis, which can also explain the complete pore blocking behavior. In the three other cases, we observed mostly the presence of micro-flocs without microsand (i.e. un-ballasted flocs).

Table 4.2: Fouling mechanisms determined with the Unified Hermia model for various water qualities on a 100 μm nylon strainer

Plant	**Type of water**	**Turbidity [NTU]**	**TSS [mg/L]**	**Fouling mechanism (best fitted model)**	**Model parameters (100 μm nylon)**	
					k_v [m^2/m^3]	**R^2**
Pont-Viau	Clarified	1.00	3.2	Standard blocking	8.36×10^{-3}	0.9857
Pont-Viau	90CW/10FW	1.02	3.0	Intermediate blocking	1.82×10^{-2}	0.9943
Pont-Viau	70CW/30FW	2.14	4.9	Cake formation	4.88×10^{-2}	0.9856
St-Damase	Clarified	0.80	1.8	Standard blocking	7.16×10^{-3}	0.9674
St-Damase	90CW/10FW	4.59	56	Complete blocking	9.07×10^{-3}	0.8480
St-Damase	70CW/30FW	10.5	164	Complete blocking	9.06×10^{-3}	0.7785
St-Damase	Flocculated	39.9	542	Complete blocking	2.03×10^{-2}	0.7829
Lévis	Clarified	1.20	4.2	Complete blocking	9.49×10^{-3}	0.9532
Lévis	90CW/10FW	4.94	22	Complete blocking	2.15×10^{-3}	0.7497
Lévis	70CW/30FW	8.83	56	Cake formation	7.33×10^{-3}	0.7843
Lévis	Flocculated	21.5	178	Cake formation	1.07×10^{-2}	0.7992
L'Assomption	Clarified	0.62	1.1	Standard blocking	2.16×10^{-3}	0.9760

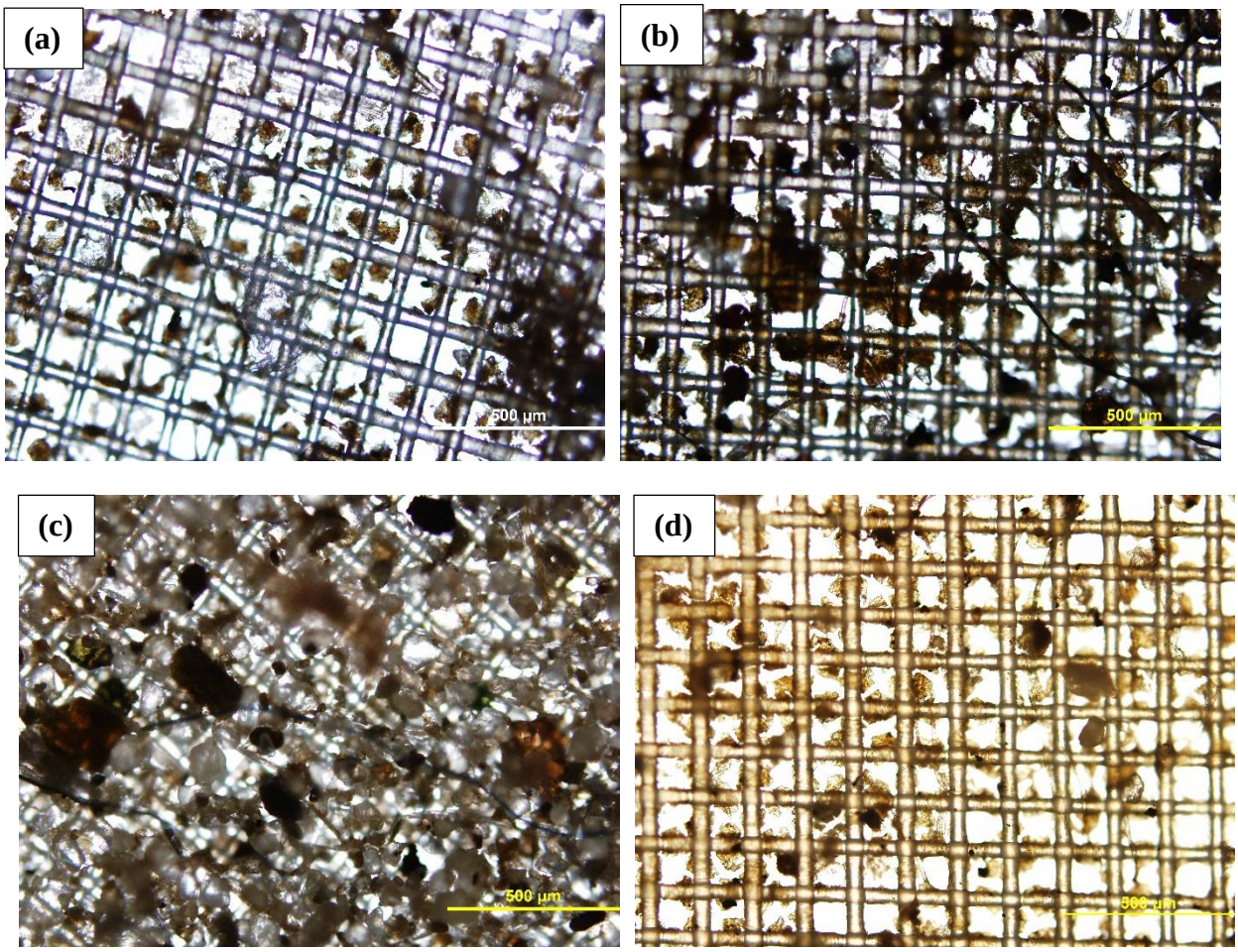

Figure 4.7: 100 µm nylon strainers clogged with clarified water from: (a) Pont-Viau, (b), Saint-Damase, (c) Lévis, and (d) L'Assomption.

Table 4.3 presents the fouling mechanisms determined for the SS strainers with different opening sizes tested on clarified waters from Actiflo® (Pont-Viau). For the 75 and 103 µm strainers, the standard pore blocking was the dominant fouling type, with some exceptions that presented an intermediate pore blocking. On the other hand, for the 152 µm strainer, the intermediate pore blocking was the dominant fouling type. Microscopy images of 75, 103, and 152 µm SS strainers clogged with clarified water are presented in Figure 4.8. In the case of 75 µm SS strainer, the standard pore blocking can be explained by the adsorption of un-ballasted flocs rather than microsand between the strainer wires, since the flocs seem to produce a pore constriction instead of blocking it completely. Although, the presence of microsand might explain an incipient intermediate pore blocking type, which was determined in some 75 µm strainers (4 of 10 assays).

In the case of 103 μm SS strainer, ballasted flocs (flocs with microsand) seems to be the main cause of the standard pore blocking, as it can be observed in Figure 4.8(b), ballasted flocs (smaller than pores) were adsorbed between the strainer wires, reducing the pore size, despite the presence of few microsands able to completely block the pores. Finally, for 152 μm SS strainer, the intermediate pore blocking can be explained by un-ballasted and ballasted flocs attached on others flocs, which, apparently, produced an increase of their size, covering most part of the pores.

Table 4.3: Fouling mechanisms determined with the Unified Hermia model for clarified water (Pont-Viau) on SS strainers

Filterability test	**Type of water**	**Strainer opening size [μm]**	**Fouling mechanism (best fitted model)**	**Model parameters**	
				k_v [m^2/m^3]	**R^2**
F1	Clarified	75	Intermediate blocking	1.45×10^{-2}	0.9942
F2			Standard blocking	1.22×10^{-2}	0.9938
F3			Standard blocking	1.25×10^{-2}	0.9932
F4			Standard blocking	1.11×10^{-2}	0.9936
F5			Standard blocking	1.04×10^{-2}	0.9911
F6			Standard blocking	8.88×10^{-3}	0.9839
F7			Intermediate blocking	1.12×10^{-2}	0.9906
F9			Standard blocking	8.14×10^{-3}	0.9948
F10			Intermediate blocking	1.36×10^{-2}	0.9951
F11			Intermediate blocking	1.51×10^{-2}	0.9964
F12	Clarified	103	Standard blocking	5.57×10^{-3}	0.9937
F13			Standard blocking	4.71×10^{-3}	0.9855
F14			Standard blocking	4.66×10^{-3}	0.9911
F15			Standard blocking	4.95×10^{-3}	0.9679
F16			Standard blocking	4.91×10^{-3}	0.9881
F18			Standard blocking	7.01×10^{-3}	0.9854
F19			Standard blocking	5.83×10^{-3}	0.9928
F20			Intermediate blocking	7.88×10^{-3}	0.9951
F21			Intermediate blocking	7.83×10^{-3}	0.9970
F22			Intermediate blocking	7.63×10^{-3}	0.9954
F23	Clarified	152	Standard blocking	2.21×10^{-3}	0.9814
F27			Intermediate blocking	3.84×10^{-3}	0.9855
F28			Intermediate blocking	3.36×10^{-3}	0.9823
F29			Intermediate blocking	3.59×10^{-3}	0.9810
F30			Intermediate blocking	3.26×10^{-3}	0.9862
F31			Intermediate blocking	3.50×10^{-3}	0.9933
F32			Intermediate blocking	2.98×10^{-3}	0.9797
F33			Intermediate blocking	2.79×10^{-3}	0.9736
F34			Intermediate blocking	2.62×10^{-3}	0.9871

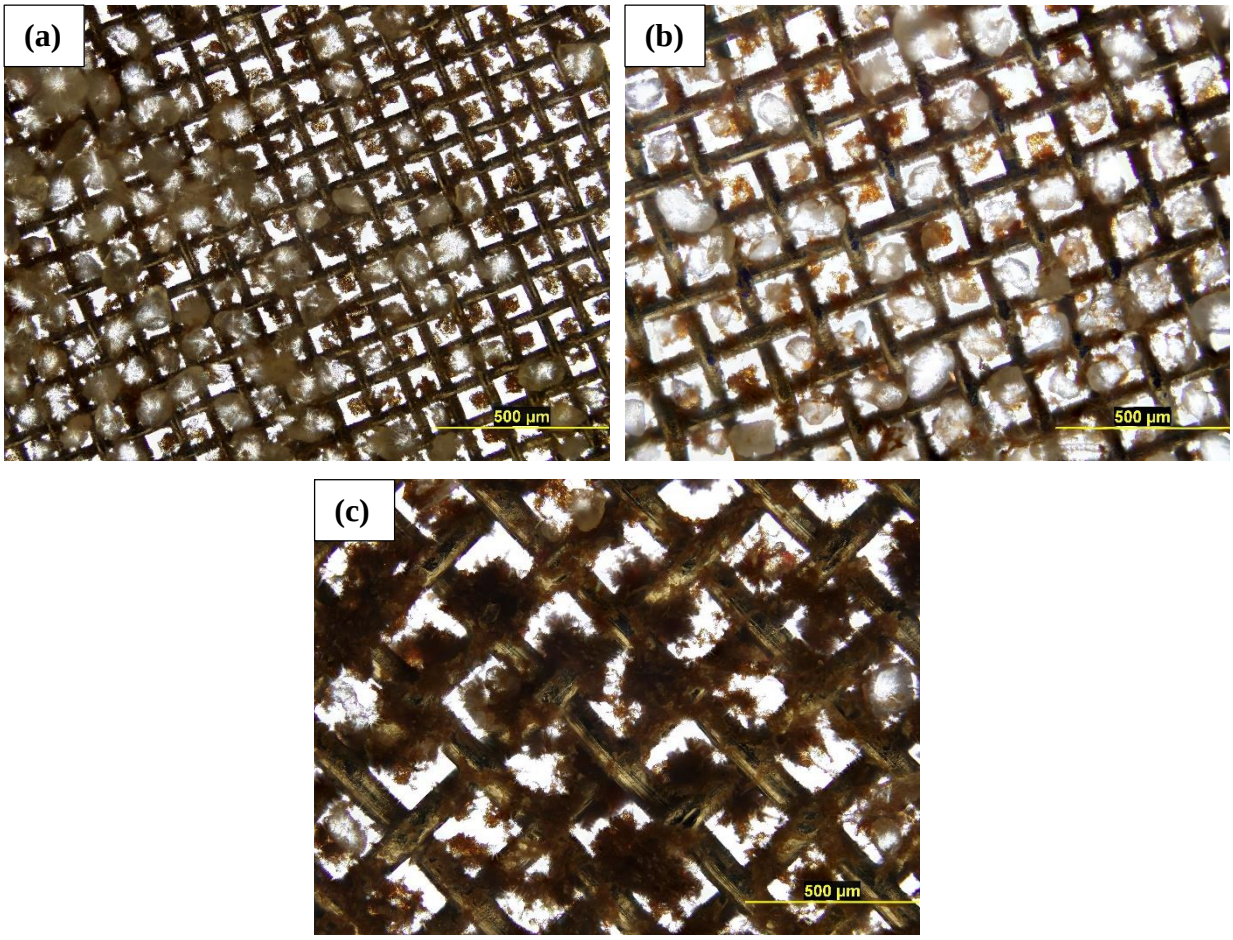

Figure 4.8: SS strainers clogged with clarified water (Pont-Viau) represented by: (a) standard blocking on 75 µm (F9), (b) standard blocking on 103 µm (F12), and (c) intermediate blocking on 152 µm (F31).

4.3.2 Prediction of fouling coefficients (k_v) based on water quality

The prediction of fouling coefficients (k_v) on microstrainers was tested based on general water characteristics. In order to determine the best relationship of the water characteristics with k_v, the Pearson correlation was used. For k_v values corresponding to a standard pore blocking of a 103 μm SS strainer (Figure 4.9 and Figure 4.10), they presented a slightly stronger correlation with total suspended solids ($r = 0.89$, $p = 0.0006$), but a weak correlation with turbidity ($r = 0.58$, $p = 0.0788$), and also a moderate correlation with particle concentration was observed ($r = 0.78$, $p = 0.0224$). In the case of k_v values predicted by a complete pore blocking model for a 100 μm nylon strainer, the insufficient data did not allow to find a correlation with the water characteristics (Figure 4.11). Although, it is possible to observe that lower and higher k_v values were obtained at very low and high values of TSS and turbidity, respectively.

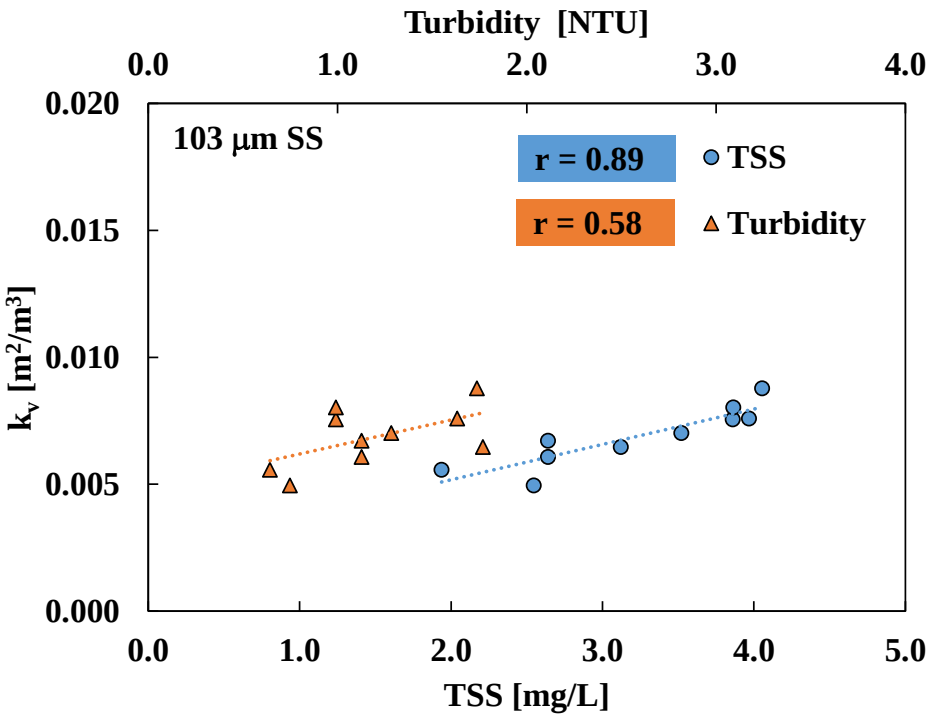

Figure 4.9: Total suspended solids (TSS) and turbidity effect on fouling coefficient (k_v) predicted by a standard pore blocking model for a 103 μm SS strainer

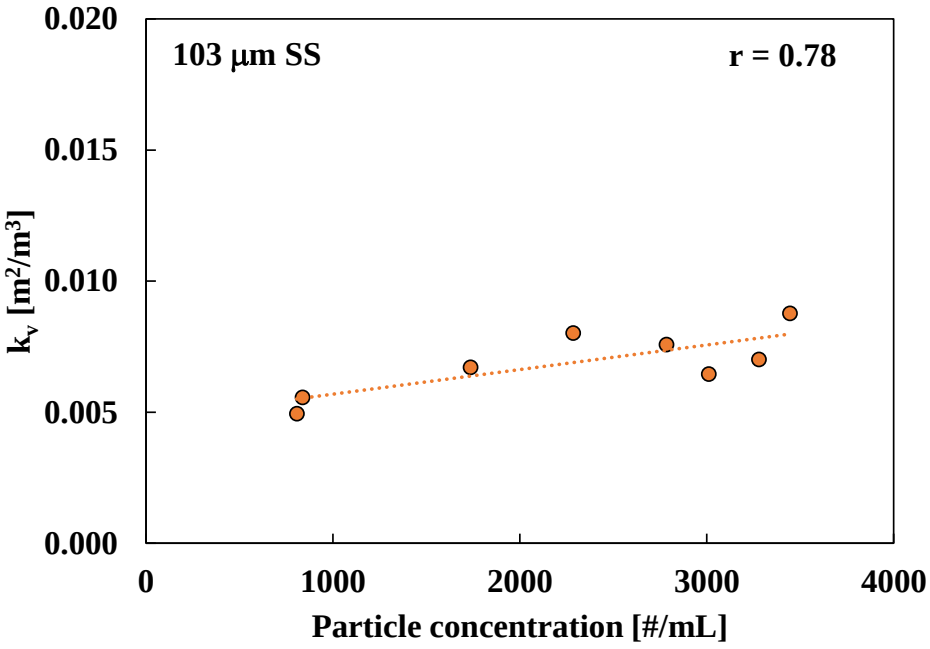

Figure 4.10: Particle concentration effect on fouling coefficient (k_v) predicted by a standard pore blocking model for a 103 μm SS strainer

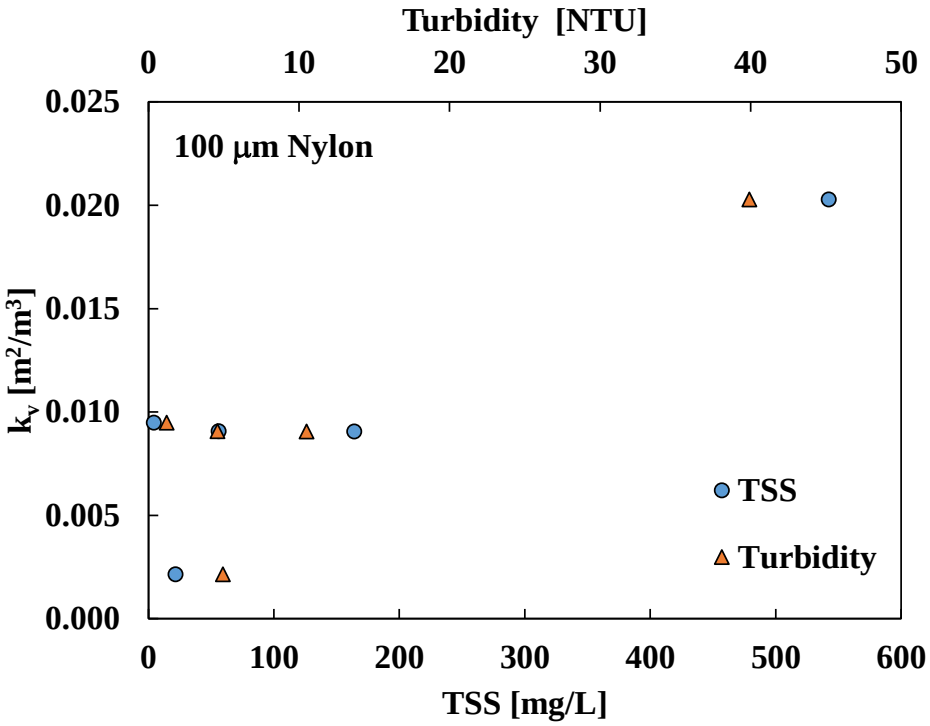

Figure 4.11: TSS and turbidity effect on fouling coefficient (k_v) predicted by a complete pore blocking model for a 100 μm nylon strainer

In stainless steel microstrainers, the relationship between the fouling coefficient (k_v) and the retained solids at the strainers per filtered volume was also studied (Figure 4.12). Each group of data, separated by the intermediate and standard pore blocking mechanisms, contains k_v values of different pore opening sizes (75, 103 and 152 μm), the distribution of the k_v values of each pore size is discussed in section 4.4.2. Despite the limited data, a significant correlation with the k_v values predicted by the intermediate pore blocking model ($r = 0.92$, $p = 0.0268$) was observed. On the other hand, a poor correlation was observed with the k_v values predicted by the standard pore blocking model ($r = 0.72$, $p = 0.1066$). Therefore, the results suggest that the k_v values represented by an intermediate pore blocking can be explained by the solids content on the microstrainers.

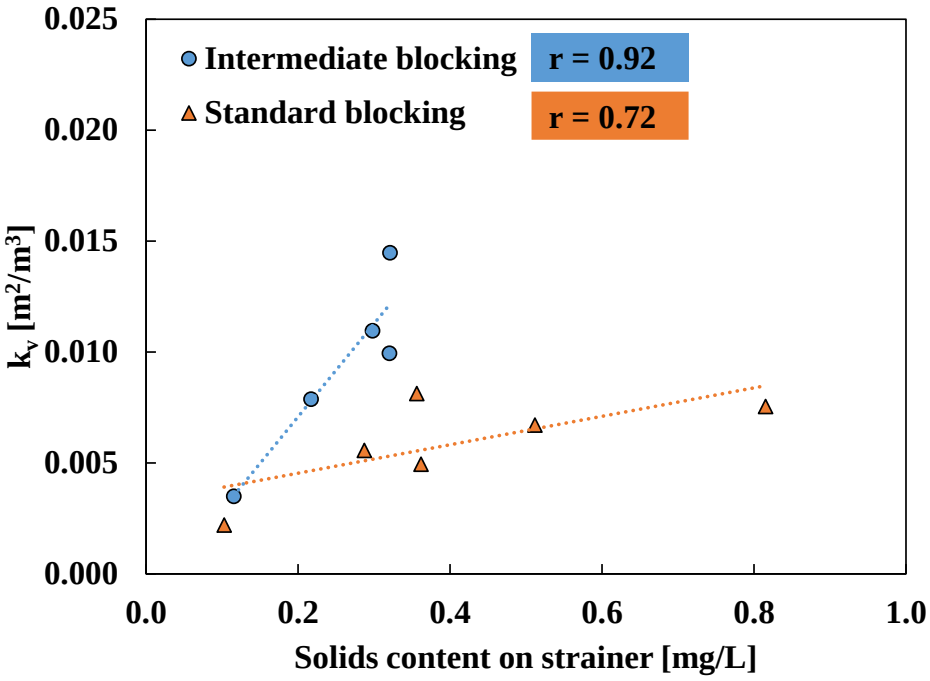

Figure 4.12: Effect on fouling coefficient (k_v) prediction by retained solids on SS strainers per filtered volume

4.3.3 Filterability index as fouling predictor

The filterability index (FI) on a 0.45 μm filter was also tested as a potential fouling predictor on microstrainers, comparing the fouling coefficients (k_v) obtained on 100 μm nylon (Table 4.2) with the FI of the different types of water. According to the plot shown in Figure 4.13, it was not possible to obtain a correlation, since k_v values involve different types of fouling mechanisms. Although, in the case of the complete pore blocking, it can be observed that low values of FI correspond to low values of k_v and a high FI value correspond to a high k_v value. The highest value of k_v was produced by a flocculated water.

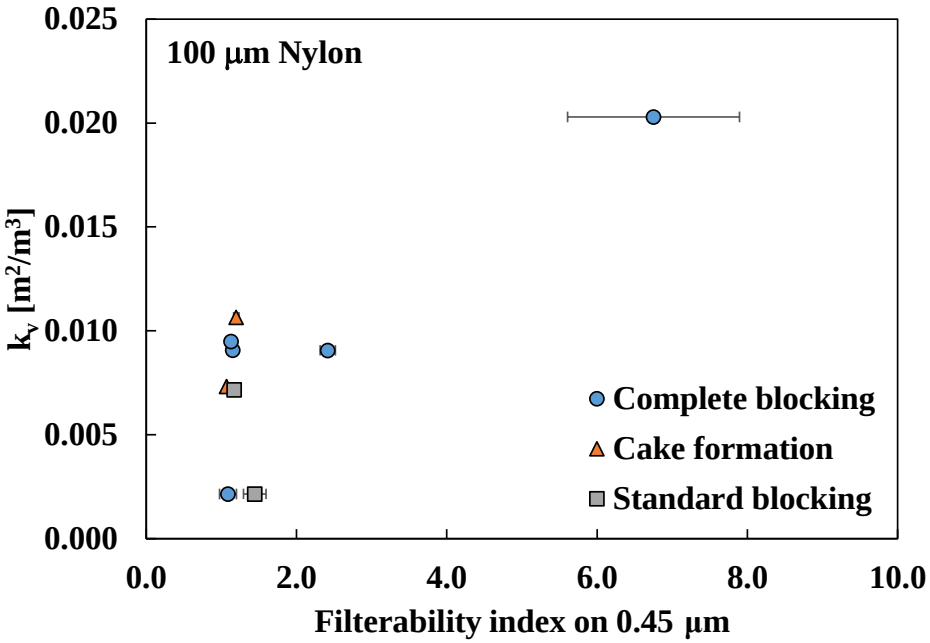

Figure 4.13: Filterability index on fouling coefficient (k_v) prediction

4.4 Impact of design/operating conditions on fouling

The different design/operating conditions that might have an effect on the type of fouling and the fouling coefficient value (k_v) on microstrainers were studied. Such design/operating conditions are the strainer material, the pore opening size and the effective velocity, which are presented in the following sub-sections.

4.4.1 Strainer material

The strainer materials used were nylon and stainless steel. The fouling on a 100 μm nylon strainer by clarified water from Pont-Viau (3.2 mg TSS/L) presented a fouling coefficient $k_v = 8.36 \times 10^{-3}$ m^2/m^3 (CV=1.2%) at 20 °C, which was described by the standard blocking mechanism. Whilst a SS strainer with a similar pore size (103 μm) and using clarified water from Pont-Viau (2.0 mg TSS/L) presented a fouling coefficient $k_v = 5.38 \times 10^{-3}$ m^2/m^3 (CV=16%) at 8.2 °C, which was also described by the standard blocking mechanism. In both materials, despite the different k_v values, the same type of pore blocking mechanism was determined at similar opening sizes but at different temperatures and TSS concentrations. Hence, it is not possible to evaluate the effect of the type of

material on the fouling coefficient, although as was discussed before, the variation of the fouling coefficient might be related to the TSS concentration (using a given strainer opening size). In addition, it is important to consider the effect of surface charge of the materials in their fouling by adsorption, especially of stainless steel which is reported to be pH dependent and it tends to be negative at neutral pH (Fukuzaki, Urano, & Nagata, 1995). It can be assumed that an electrostatic attraction might not occur or it is negligible between residual flocs (polymer particularly) of the clarified water and the SS strainer, since clarified water has a negative SCV and pH near neutrality. However, this requires to be studied in a further research.

4.4.2 Pore opening size

Based on data of Table 4.3, the fouling coefficient (k_v) values can be distinguished by each pore size of the SS strainers (Figure 4.14). The fouling coefficients value is affected by the pore size of the strainers, where for a smaller pore size, the higher will be the fouling coefficient; and for a bigger pore size, the lower is the fouling coefficient. For 75 μm strainer, k_v ranged between 0.008 and 0.015 m^2/m^3. For 103 μm strainer, k_v ranged between 0.005 and 0.008 m^2/m^3. In the case of 152 μm strainer, k_v ranged between 0.002 and 0.004 m^2/m^3. The coefficient of variation on k_v were 19%, 22% and 17% for the 75, 103 and 152 μm strainers, respectively. The variability in k_v values also followed a normal probability distribution (Appendix E).

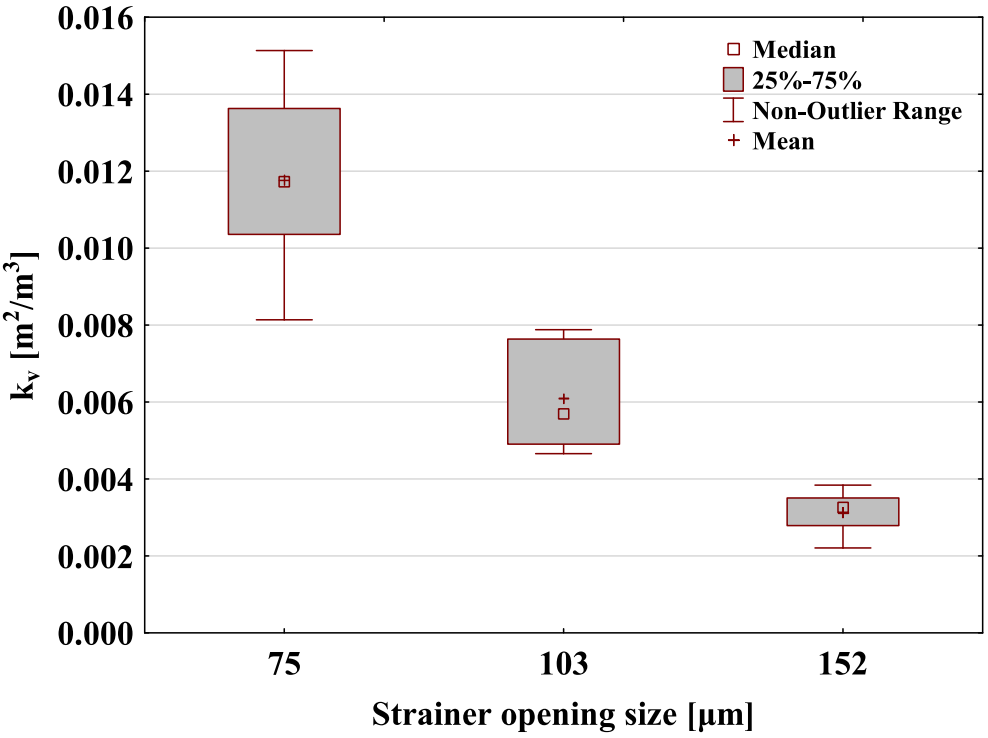

Figure 4.14: Fouling coefficient (k_v) values according to SS strainer opening size. T= 8.2 °C

4.4.3 Effective velocity

The effective velocity will change according to the open area (or effective filtration area) of each strainer, applying a same approach velocity (0.08 m/s). The effective velocity for each SS strainer is indicated in Table 4.4. There is a small difference between the respective effective velocities and it is not expected to have a significant impact on fouling behavior. As was mentioned above, the pore size is the most important design/operational parameter in the type of fouling.

Table 4.4: Effective velocity according to microstrainer open area

Strainer opening size [µm]	Open area [%]	Approach velocity [m/s]	Effective velocity [m/s]
75	46	0.08	0.17
103	37		0.22
152	38		0.21

4.5 Impact of operating conditions on backwashing

The effect of different backwashing factors on solids removal at SS strainers were studied, which includes pore opening size, backwash velocity, chlorine concentration, and pH. Chlorine concentration was adjusted with diluted sodium hypochlorite while pH was adjusted with sodium hydroxide. The interactive (factorial) and non-interactive (or main effects) ANOVA was carried out to discriminate the impacts of each variable.

According to the factorial ANOVA of parameters (strainer opening size, backwash velocity and pH), there is a significant effect of each parameter on the solids removal, where pH was found to have the most important effect on solids removal, followed by the backwash velocity. However, there is not a significant effect on solids removal by the interaction of such parameters (Figure 4.15, 4.16, and 4.17), although it can be observed certain influence of a high BW velocity (0.35 m/s) at pH 11 (Figure 4.17). See detailed results of factorial ANOVA in Appendix F. A detailed discussion of the main effects ANOVA results are presented in the following sub-sections, which also include the oxidizing condition with chlorine.

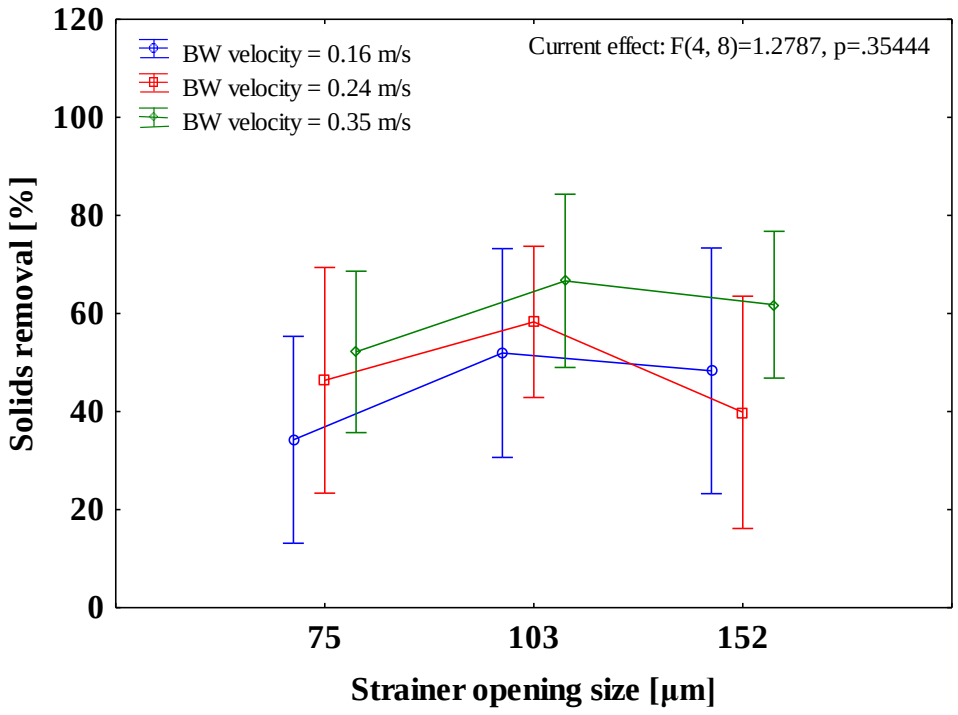

Figure 4.15: Interaction effect of strainer opening size and BW velocity on solids removal

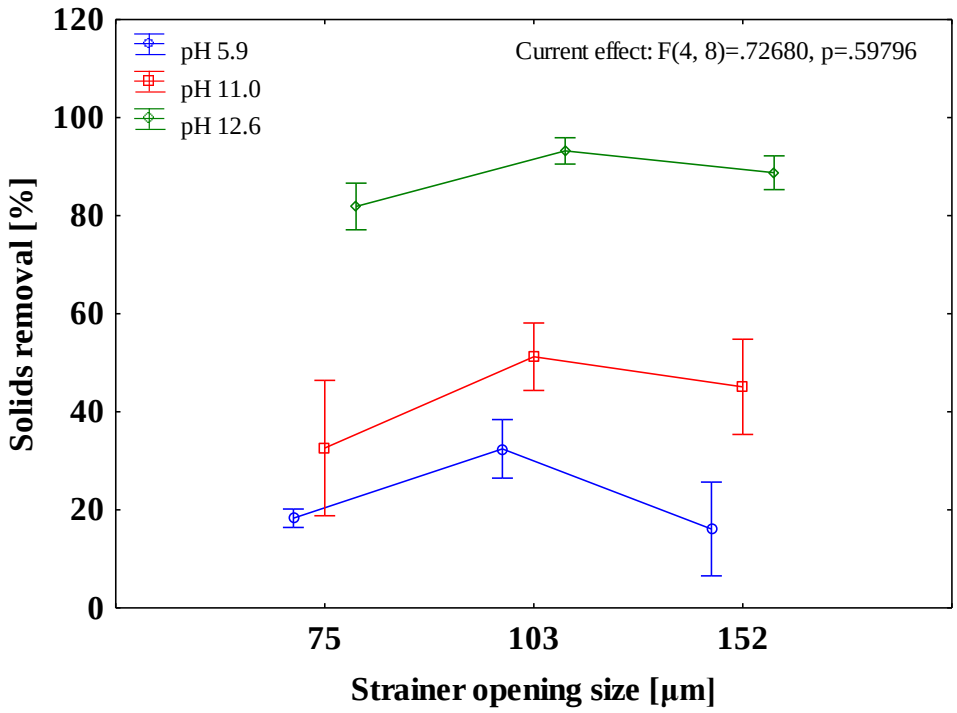

Figure 4.16: Interaction effect of strainer opening size and pH on solids removal

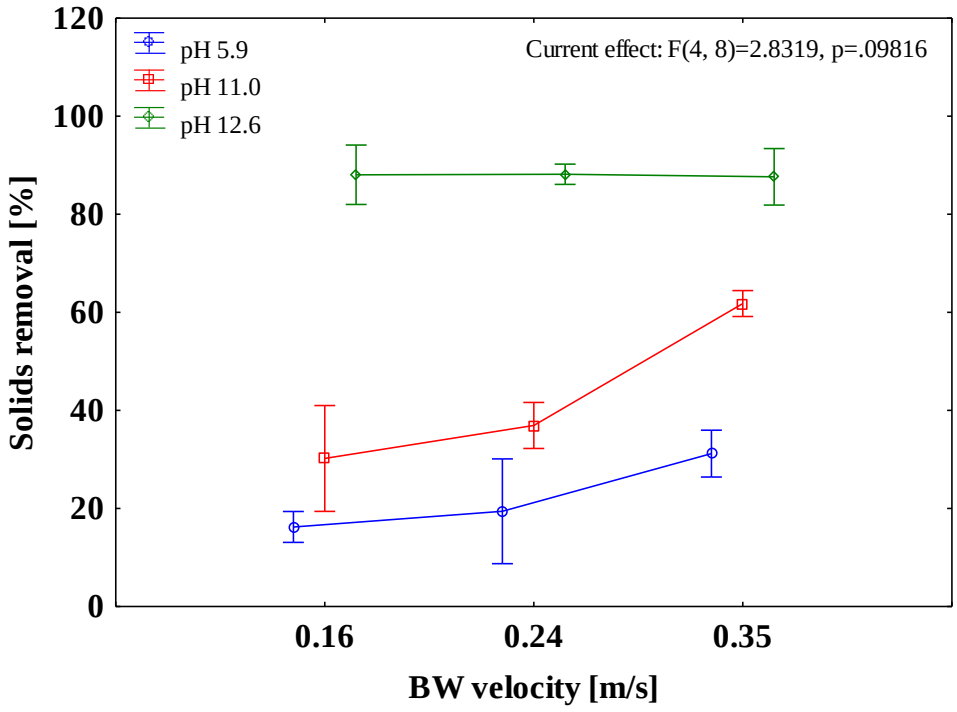

Figure 4.17: Interaction effect of BW velocity and pH on solids removal

4.5.1 Pore opening size

The solids removal results based on strainer opening size are presented in Figure 4.18. The mean values of solids removal for 75, 103 and 152 µm were 37.3%, 49.8%, and 50.0%, respectively. These results include the backwashing tests performed with filtered water, oxidizing (chlorine) and alkaline (NaOH) reagents.

The pore opening size has a significant effect on solids removal after backwashing (p=0.005), where 103 and 152 µm strainers statistically presented a higher solids removal than the 75 µm strainer. Although, there is no significant difference in the solids removal between 103 and 152 µm strainers (see ANOVA results in Appendix G).

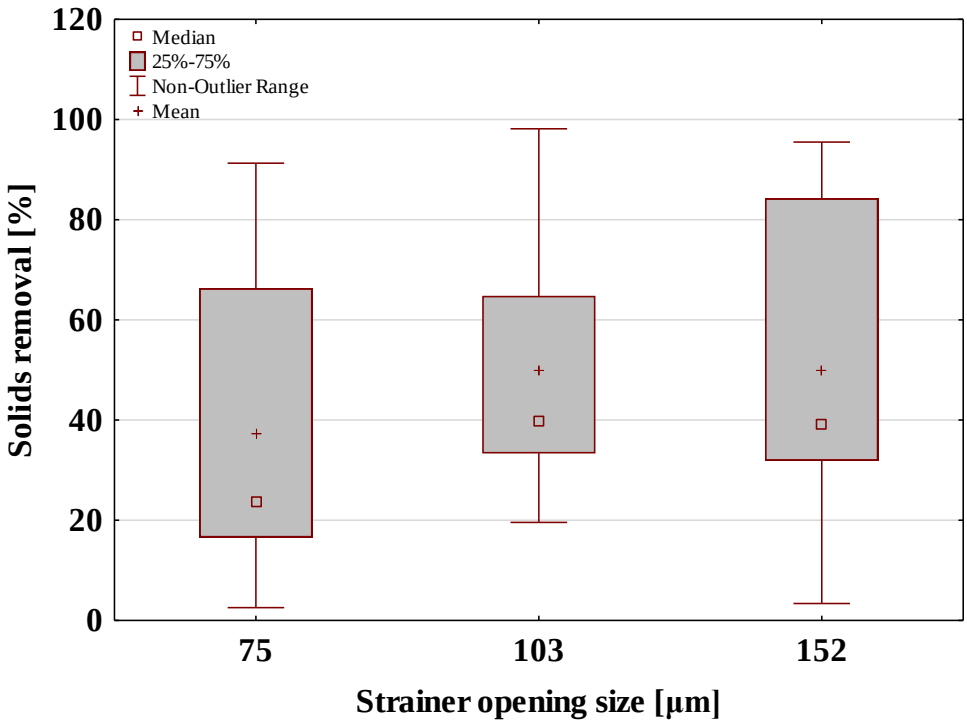

Figure 4.18: Solids removal after backwashing according to strainer opening size

4.5.2 Backwash velocity

The results of solids removal by varying the backwash velocity are presented in Figure 4.19. The mean values of solids removal for BW velocities of 0.16, 0.24, and 0.36 m/s were 39.1%, 41.0%, and 60.2%, respectively.

Statistically, the BW velocity has a significant effect on solids removal (p=0.00658), especially the higher BW velocity (0.35 m/s), which produced a higher solids removal than the other two velocities. In addition, no significant difference in the effect of the two lower velocities was observed (see ANOVA results in Appendix G).

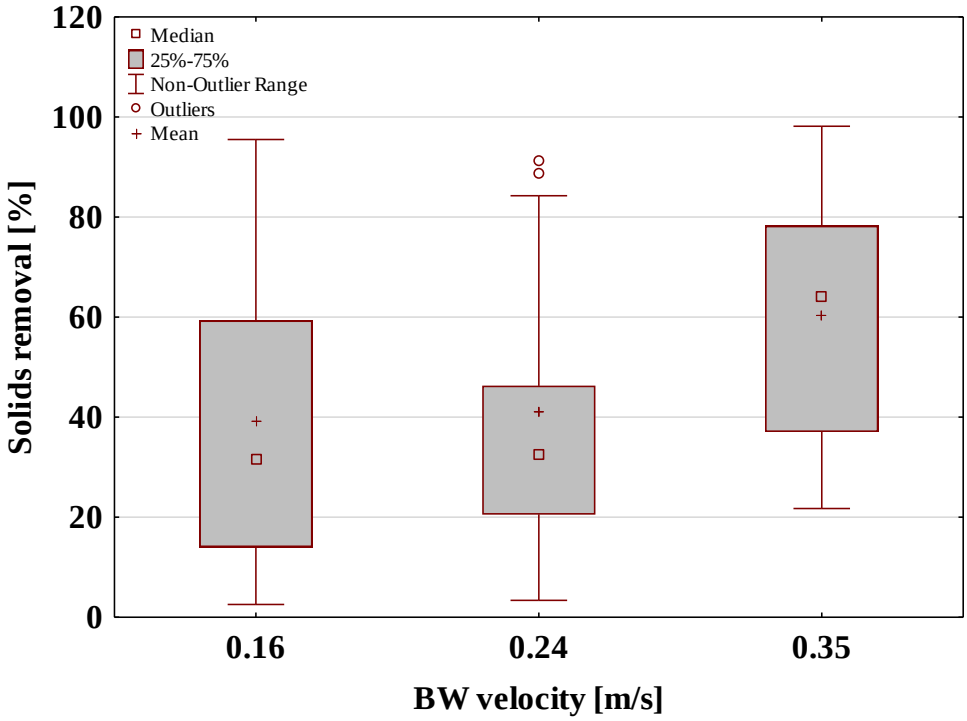

Figure 4.19: Solids removal after backwashing according to backwash velocity

Regarding the type of flow regime produced by the three BW velocities through the SS strainers with a plain square weave, an estimation of the wire Reynolds number (Re_d) was determined (Azizi & Al Taweel, 2011). Re_d is defined in terms of the wire diameter and the approach velocity. It assumes the *flow-around* submerged objects (wires). Then Re_d was normalized by the open area of the strainers (Re_d/β), in order to include the effective velocity rather than the approach velocity (Chhabra & Richardson, 1985). The Re_d/β obtained for the different SS strainers are presented in Table 4.5 (water density = 999.84 kg/m^3, dynamic viscosity = 1.33x10^{-3} kg/m·s). According to Chhabra and Richardson (1985), all three BW velocities applied through the SS strainers produce a certain turbulence ($Re_d/\beta > 5$). Although, a strong turbulent flow through screens is generally observed at $Re_d/\beta > 100$ (Azizi & Al Taweel, 2011; Chhabra & Richardson, 1985). This might

explain the small increase of solids removal at high BW velocity (0.35 m/s) using only filtered water at pH 5.9 (see Figure 4.17).

Table 4.5: Normalized Reynolds number (Re_d/β) at various BW velocities through SS strainers

Strainer opening size [μm]	**Open area, β [%]**	**Wire diameter [mm]**	**BW velocity [m/s]**	**Re_d**	**Re_d/β**
75	46	0.0356	0.16	4	9
			0.24	6	14
			0.35	9	21
103	37	0.0660	0.16	8	21
			0.24	12	32
			0.35	18	47
152	38	0.1016	0.16	12	32
			0.24	18	48
			0.35	27	71

4.5.3 Effect of pH

The effect of pH in backwashing was evaluated under all conditions, which include a filtered water (pH 5.9), oxidizing solution (10 and 100 ppm of chlorine, corresponding to pH 8.0 and 9.4, respectively), and alkaline solution by addition of NaOH (pH 11.0 and 12.6). The solids removal obtained by these conditions are presented in Figure 4.20. The mean values of solids removal according to pH of the backwash solution were 22.3%, 21.4%, 26.5%, 43.0%, and 88.0% for pH 5.9, 8.0, 9.4, 11.0, and 12.6, respectively. Statistically, pH provided a significant effect ($p \leq 0.00001$) on solids removal, which was mostly influenced by the pH values of the high alkaline conditions (pH 11.0 and 12.6). On the other hand, no significant effect on solids removal of pH values under oxidizing conditions was observed, in other words, by increasing chlorine concentration up to 100 ppm, there is no significant effect in backwash efficiency. Backwashing with only filtered water also seems to have no significant effect in solids removal (see ANOVA results in Appendix G). An example of the pH effect of filtered water and alkaline condition on the 75 μm strainer backwashing is presented in Figure 4.21, in which it can be observed the difference of clean area after the first BW cycle at 0.35 m/s. For pH values 5.9 and 12.6, a clean area of 47.0% and 84.2% after the first BW were determined, respectively.

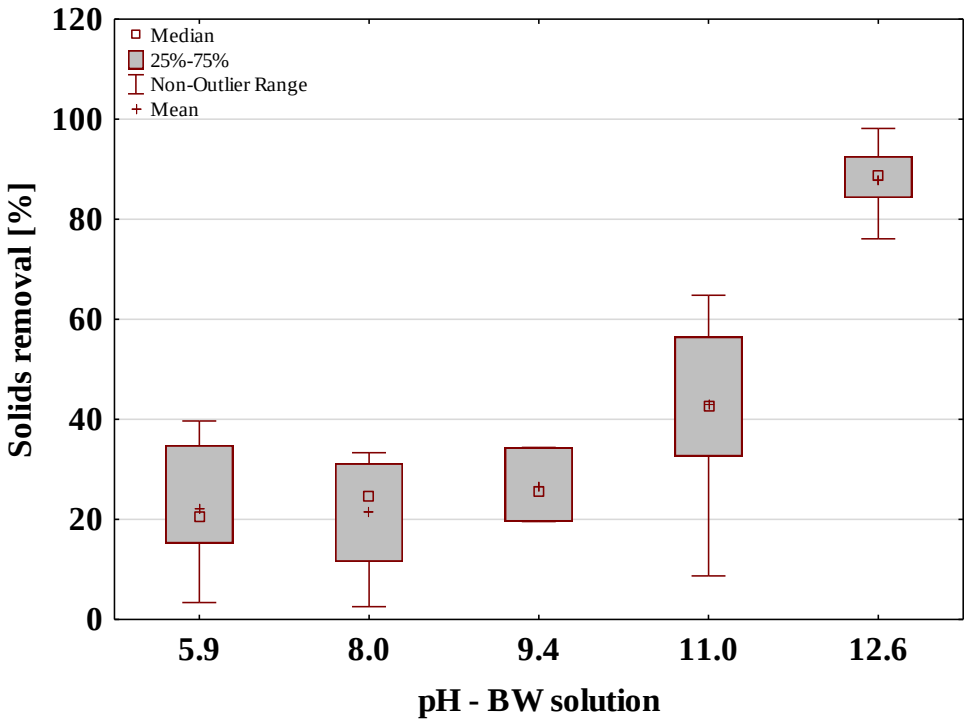

Figure 4.20: Solids removal after backwashing according to pH

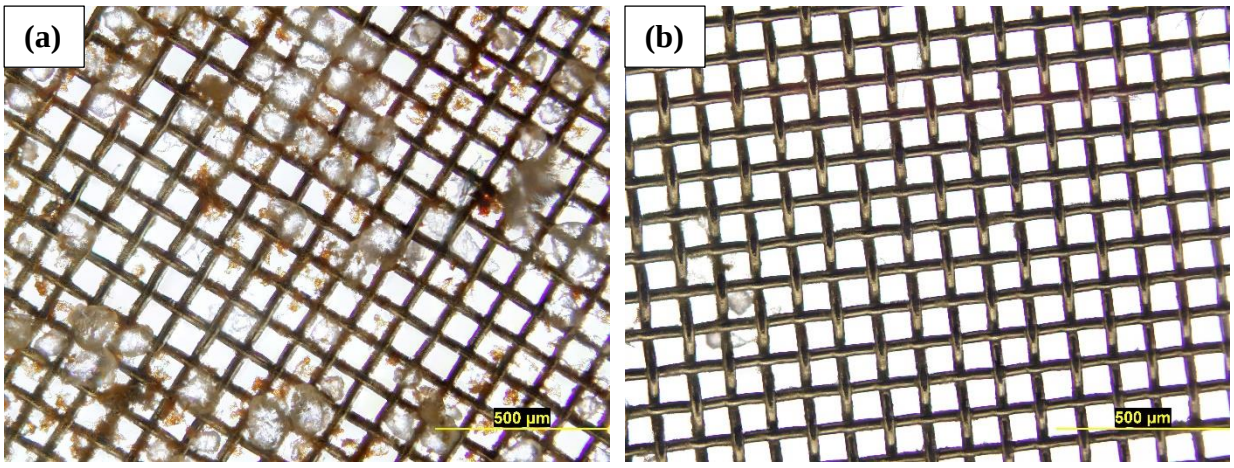

Figure 4.21: Effect of pH after the first backwash cycle on 75 µm SS strainer. (a) pH 5.9 and (b) pH 12.6

The effectiveness of a strong alkaline condition (pH 12.6; 0.045 N NaOH) and high BW velocity (0.35 m/s) on backwashing it was also evaluated after various (5) backwash cycles on the 75 µm strainer (Figure 4.22). Filterability was performed with clarified water of Pont-Viau. At pH 12.6, the filterability tests lasted between 20 and 22 min (first test lasted 22 min) and the specific filtered volume (or productivity) ranged between 94 and 105 m^3/m^2, with a maximum reduction of productivity of about 10%. Comparing these results with a BW solution at pH 5.9 (filtered water) using the same high BW velocity, the filterability tests lasted between 2.3 and 20 min (first test lasted 20 min) and the specific filtered volume ranged between 11 and 94 m^3/m^2, with a maximum reduction of productivity of about 88%. Therefore, these results confirmed that the effect of a high pH value is more significant than the effect of a high BW velocity on backwashing.

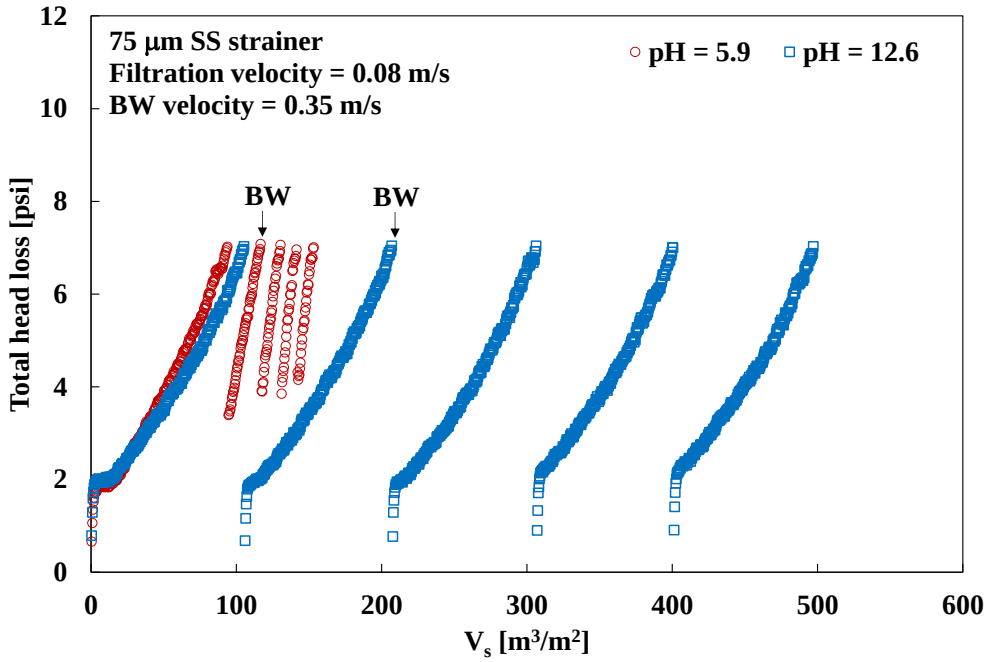

Figure 4.22: Filterability test performance after various backwashing cycles

4.6 Water consumption for backwashing

The backwashing performance on the different SS strainers was also evaluated from the standpoint of backwashing water consumption regarding the produced water during the filterability tests (Table 4.6). As expected, there is a high percentage of BW water usage at the highest BW velocity

(0.35 m/s) for each strainer opening size. The lower percentages of BW water usage can be observed on the 152 μm strainers (< 20%), since they produced larger water volumes when reaching 7-psi head loss (head loss recommended to trigger backwashing). Thus, one of the advantages of using larger strainers is that the water consumption for BW is very low compared to the productivity during filtration.

Table 4.6: BW water consumption regarding the produced water using SS strainers

Strainer opening size [μm]	Produced water volume (at ΔP = 7 psig) [L]	BW velocity [m/s]	BW water usage (for 5 min) [L]	BW volume/produced water volume [%]
75	11	0.16	3.0	28
	9	0.24	4.5	52
	9	0.35	6.8	78
103	17	0.16	3.0	17
	16	0.24	4.5	29
	14	0.35	6.8	47
152	37	0.16	3.0	8.2
	38	0.24	4.5	12
	38	0.35	6.8	18

4.7 Infrared spectrum of polymer

Characteristic peaks of commercial APAM (Hydrex 3511) in a pure dry state were identified on IR spectrum (Figure 4.23), according to Yi et al. (2012); Stuart (2005). The asymmetric and symmetric stretching vibration of C=O in carboxylate groups occurs at 1649 cm^{-1}, the N–H bending vibration occurs at 1609 cm^{-1}, the C–N bending occurring at 1448 cm^{-1}. The N–H stretching vibration is observed at 3331 cm^{-1}. The aliphatic C–H stretching band occurs at 2933 cm^{-1}. Additionally, in Figure 4.23 it is presented the IR spectra on 75 μm SS strainers, when it is initially clean, when it is clogged after a filterability test with clarified water (from Pont-Viau), and after backwashing at pH 5.9 and 12.6. The clogged and backwashed at pH 5.9 strainers presented the same bands, where it is possible to identify a small presence of APAM at some bands (1649 cm^{-1} and 1448 cm^{-1}). Furthermore, a high peak at 2933 cm^{-1} was observed (spectra A, B and C),

this peak was enhanced possibly due to the presence of natural organic matter (NOM) in the water, such as humic substances with aliphatic components (Lin, Liu, & Hao, 2001) which were entrapped into the flocs. The backwashed strainer at pH 12.6 did not present peaks at 1649 and 1609 cm^{-1} of C=O and N-H vibration, respectively. This result suggests that some amide groups of APAM may have been hydrolyzed under strong basic conditions (by addition of the hydroxide OH^-), producing the removal of ammonia (NH_3) (Ma et al., 2015). Despite this, the backwashing was not completely effective in this strainer since it still had the presence of some peaks such as the aliphatic chains (C–H peak at 2933 cm^{-1}).

On the other hand, the IR spectra for the 103 μm SS strainers (Figure 4.24), presented a difference in peak bands between the clogged strainer and the backwashed strainers. For this strainer, there is a clear reduction of the organic compounds (among them APAM in flocs) after backwashing at pH 5.9. As well, a further reduction was achieved by the backwashing at pH 12.6. In the case of IR spectra for the 152 μm SS strainers (Figure 4.25), there is also a very small presence of APAM at the clogged strainer (1649 cm^{-1} and 1448 cm^{-1} bands), and at the backwashed strainers these peaks decreased slightly.

Despite the important presence of aliphatic compounds from NOM in flocs presented in the three clogged strainers, it is possible to detect the presence of APAM at low peaks at 1649 cm^{-1} and 1448 cm^{-1}. According to these results, the organic compounds of the un-ballasted flocs, which are the polymer and NOM, are an important cause of pore clogging at the strainers, since after the backwashing even at high pH there was still the presence of such compounds. However, this method (FTIR) was not able to detect the inorganic compounds of the flocs (particulate aluminum), thus it was not possible to distinguish the role of the coagulant (alum) in the strainer clogging. Finally, the backwashing seems to have been more effective in the flocs removal at the 103 μm SS strainers.

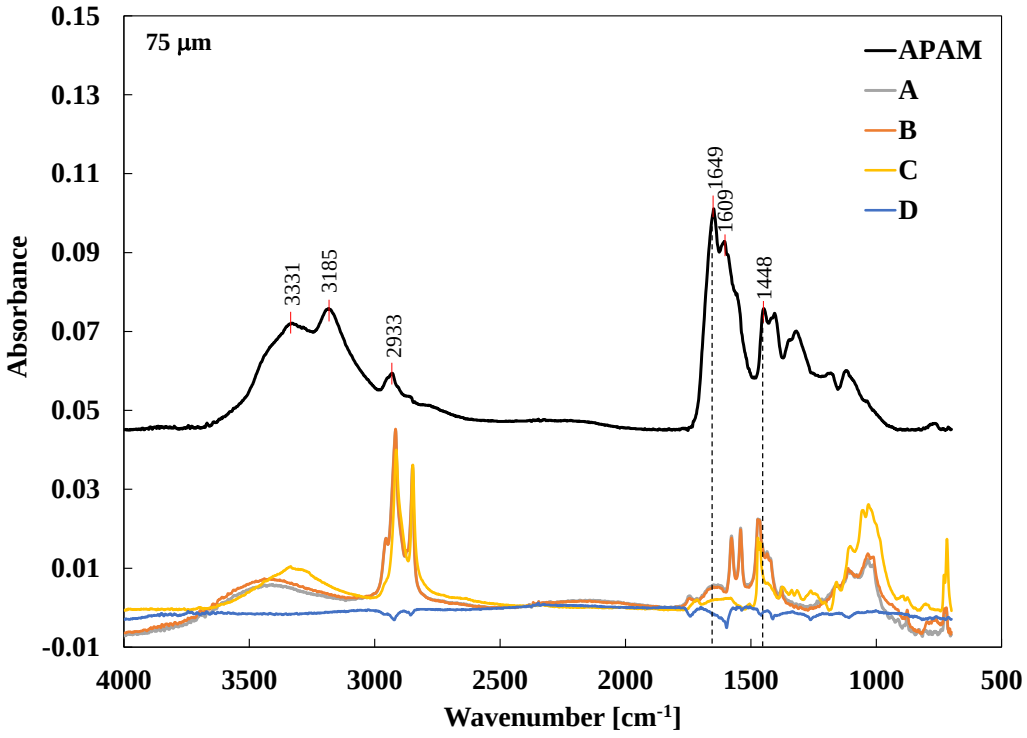

Figure 4.23: IR spectra of pure dry APAM and 75 µm SS strainers. (A) Clogged strainer, (B) strainer after BW at pH 5.9, (C) strainer after BW at pH 12.6, and (D) clean strainer

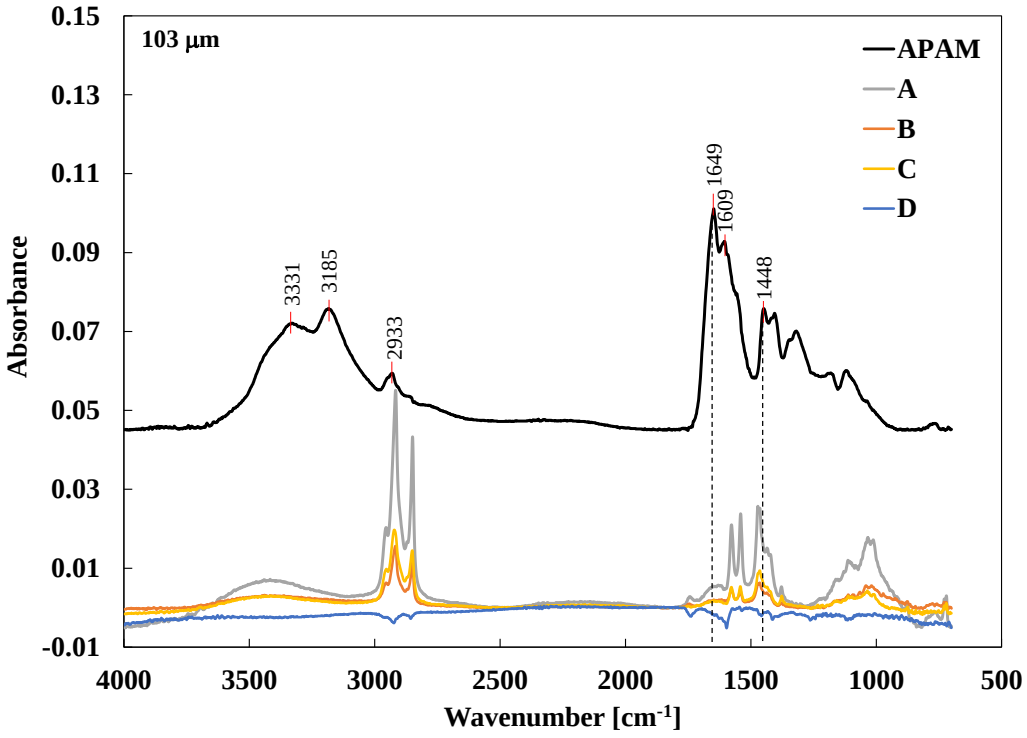

Figure 4.24: IR spectra of pure dry APAM and 103 µm SS strainers. (A) Clogged strainer, (B) strainer after BW at pH 5.9, (C) strainer after BW at pH 12.6, and (D) clean strainer

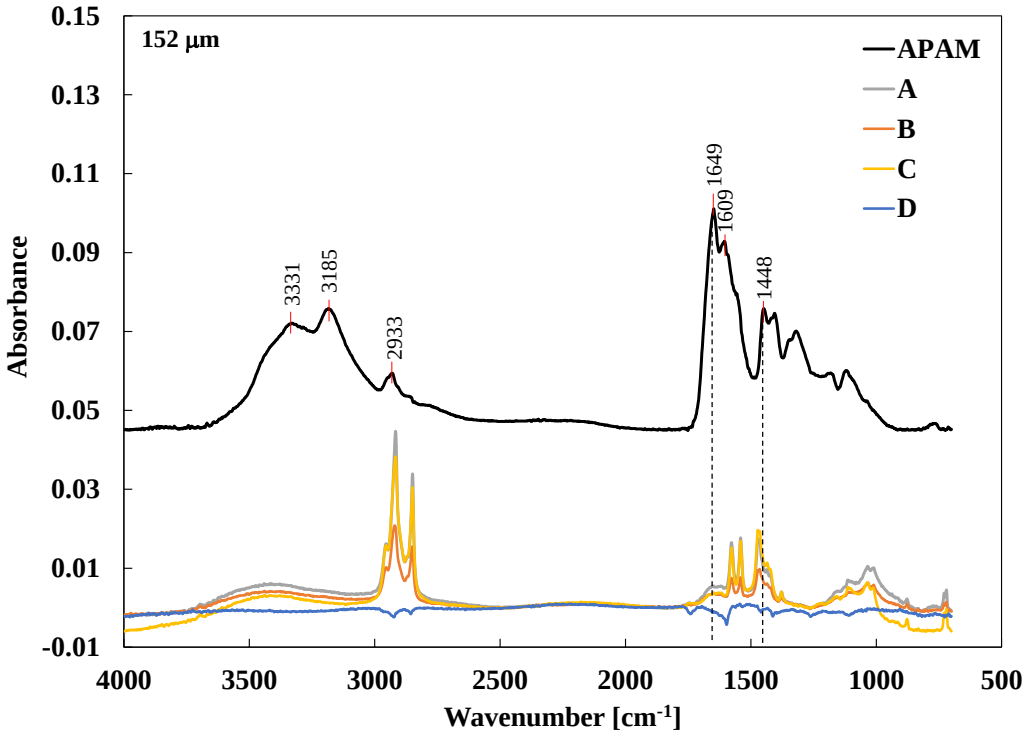

Figure 4.25: IR spectra of pure dry APAM and 152 µm SS strainers. (A) Clogged strainer, (B) strainer after BW at pH 5.9, (C) strainer after BW at pH 12.6, and (D) clean strainer

CHAPTER 5 CONCLUSIONS AND RECOMMENDATIONS

The purpose of this research project was to identify the causes of microstrainers clogging fed by an Actiflo® process and study the impact of different operational conditions on backwashing efficiency at microstrainers. In this context, the following conclusions and recommendations were drawn:

The settled (or clarified) waters collected from Actiflo® process of four drinking water treatment facilities of the province of Québec (Pont-Viau, Saint-Damase, Lévis, and L'Assomption) presented a certain potential fouling on microstrainers in the laboratory assays.

Fouling of microstrainers

The fouling mechanisms on nylon and stainless steel microstrainers produced by the four settled waters (mentioned above) can be determined by the Unified Hermia model. For a 100 μm nylon strainer, the model fitted very well ($R^2 > 0.95$) for the four settled waters qualities (TSS < 4.5 mg/L). The standard pore blocking was the dominant fouling mechanism for three settled waters (Pont-Viau, Saint-Damase, and L'Assomption), caused mainly by small un-ballasted flocs (microsand was negligible) with the exception of a complete pore blocking produced by Lévis settled water, caused by ballasted flocs (microsand was visible). In the case of lower water qualities (TSS > 20 mg/L), the model did not fit well. Regarding the fouling on SS strainers produced by settled water from Pont-Viau, the performance of the Unified Hermia model was excellent ($R^2 > 0.97$). The standard pore blocking was the dominant fouling mechanism for the 75 and 103 μm SS strainers, caused mainly by ballasted flocs, where microsand has an important effect in pore clogging, and the intermediate pore blocking was the dominant fouling mechanism for the 152 μm SS strainer, caused mainly by un-ballasted flocs agglomeration. Therefore, both microsand and polymer, integrated into the flocs, have an important effect on the type of fouling mechanism at microstrainers. At lower opening sizes the ballasted flocs are the main cause of pore clogging, while at higher opening sizes are the un-ballasted flocs. It is possible to assume that larger strainers (≥150 μm) will initially present a fouling by small un-ballasted flocs that after a certain filtration time will be agglomerated and be able to retain the exported microsand. The fouling coefficients (k_v) obtained from the model are affected by the pore size of the strainers. For a smaller pore size,

the higher will be the fouling coefficient; and for a bigger pore size, the lower is the fouling coefficient.

The total suspended solids might be a good predictor of the fouling coefficient (k_v), since it presented a fairly strong correlation with the fouling coefficient corresponding to the standard pore blocking mechanism at the 103 µm SS strainer. However, its use is limited to low TSS concentrations and the correlation might vary depending of the strainer opening size. A second possible predictor is the particle concentration, which presented a moderate correlation with the fouling coefficient. Another method that might be useful to predict the k_v values (for an intermediate pore blocking) is by the solids content at the microstrainers (in mg/L). On the other hand, turbidity is a poor predictor since it was unable to detect the microsand (one of the causes of pore clogging), which settles rapidly. Filterability index (FI) performed on a 0.45 membrane had no prediction ability of the fouling coefficient for a specific pore blocking mechanism.

Most UF/MF membrane manufacturers recommend to use strainers with openings larger than 200 µm ahead of their system. Based on our results, we recommend that strainers used to pre-filtered Actiflo® settled waters prior to UF/MF should also be above 200 µm. On one hand, some may argue that using a lower opening size would offer a protection against a sudden export of microsand due to an improper operation of the Actiflo. Our opinion is to the effect that a sudden microsand export would be captured by a 200 µm strainer even if the microsand has an effective size lower than this value. In practice, a microstrainer operating under a high TSS loading will rapidly produce cake formation. The cake porosity is lower than the opening size and will capture microsand. Therefore, the opening size of the microstrainer should be selected to have the small ballasted flocs transit through the microstrainer and be captured on the UF/MF membranes. The concentration of microsand exported during normal operation of an Actiflo® is low (1-2 mg/L). Such concentration can be properly eliminated by the membranes, which are able to handle much higher TSS.

Backwashing at microstrainers

Regarding the backwashing of microstrainers, the pH of a cleaning solution has a significant effect on backwashing efficiency (about 88% of solids removal), especially under strong alkaline conditions (pH > 11.0), which most likely promotes hydrolysis of residual polymer and dissolution of particulate aluminum. A second important factor is the backwash velocity, which has a significant effect on backwash efficiency (about 60% of solids removal) at a high BW velocity

(0.35 m/s), enhancing the solids removal at pH 11.0. Thus, a BW velocity at least four times the filtration velocity is recommended. It would be desirable to test if the duration of the BW can be reduced from 5 to 1 minute in order to reduce water losses. The strainer opening size had a less significant effect on backwashing (about 50% of solids removal) for the pore sizes of 103 and 152 μm. The 75 μm strainer presented only 37% solids removal.

Finally, further studies should test if other type of polymer (e.g. activated starch) could alleviate the fouling on microstrainers. It would also be of interest to differentiate the role of alum from polymer in the formation of fouling.

BIBLIOGRAPHY

AMIAD Water Systems. (1998). Screen Filtration Technology as Applied to Pretreatment of Reverse Osmosis and Ultra-Filtration Systems Retrieved from http://www.amiad.com/pdf/articles/Screen_Filtration_Technology_as_Applied_to_Pretreatment_of_Reverse_Osmosis_and_Ultra-Filtration_Systems.pdf

AMIAD Water Systems. (2005). Removing Solids with Automatic Self-Cleaning Filters Retrieved from http://www.amiad.com/pdf/articles/removing_solids_with_automatic_self-cleaning_filters.pdf

AMIAD Water Systems. (2016). Products - EBS Filters. Retrieved from http://www.amiad.com/catalog.asp?type1=1&cat=9

APHA, AWWA, & WEF. (2012). *Standard Methods for the Examination of Water and Wastewater* (22nd ed.): American Public Health Association.

Azizi, F., & Al Taweel, A. M. (2011). Hydrodynamics of Liquid Flow through Screens and Screen-Type Static Mixers. *Chemical Engineering Communications, 198*(5), 726-742. doi:10.1080/00986445.2011.532748

Baudin, I., & Fabre, A. (2006). Optimisation des procédés de clarification : Utilisation des polymères cationiques. Retrieved from http://www.eau-seine-normandie.fr/fileadmin/mediatheque/Dossier_partage/ETUDES-Logo/Rapports/06AEP08.pdf

Blumenschein, C. D., Latker, E., & Banerjee, K. (2006). Sand Ballasted High Rate Clarification Process for Treatment of Process Water. *IWC, 6*, 20.

BOLLFILTER Protection Systems. (2015). Brochures - Product Overview. Retrieved from https://www.bollfilter.com/fileadmin/bollfilter/downloads/prospekte/Produktprogr_eng.pdf

Bolto, B. (2005). Reaction of chlorine with organic polyelectrolytes in water treatment: A review. *Journal of Water Supply: Research and Technology - Aqua, 54*(8), 531-544.

Bolto, B., & Gregory, J. (2007). Organic polyelectrolytes in water treatment. *Water research, 41*(11), 2301-2324. doi:http://dx.doi.org/10.1016/j.watres.2007.03.012

Brehant, A., Bonnelye, V., & Perez, M. (2002). Comparison of MF/UF pretreatment with conventional filtration prior to RO membranes for surface seawater desalination. *Desalination, 144*(1), 353-360. doi:http://dx.doi.org/10.1016/S0011-9164(02)00343-0

Chellam, S., & Cogan, N. G. (2011). Colloidal and bacterial fouling during constant flux microfiltration: Comparison of classical blocking laws with a unified model combining pore blocking and EPS secretion. *Journal of Membrane Science, 382*(1–2), 148-157. doi:http://dx.doi.org/10.1016/j.memsci.2011.08.001

Cheng, Y.-L., Lee, D.-J., & Lai, J.-Y. (2011). Filtration blocking laws: Revisited. *Journal of the Taiwan Institute of Chemical Engineers, 42*(3), 506-508. doi:http://dx.doi.org/10.1016/j.jtice.2010.09.004

Cheryan, M. (1998). Ultrafiltration and Microfiltration Handbook (Vol. 2nd --). Boca Raton, Fla: CRC Press.

Chhabra, R. P., & Richardson, J. F. (1985). Flow of liquids through screens: Relationship between pressure drop and flow rate. *Chemical Engineering Science, 40*(2), 313-316. doi:http://dx.doi.org/10.1016/0009-2509(85)80072-5

Desjardins, C., Koudjonou, B., & Desjardins, R. (2002). Laboratory study of ballasted flocculation. *Water research, 36*(3), 744-754. doi:http://dx.doi.org/10.1016/S0043-1354(01)00256-1

Desjardins, R. (1997). *Le traitement des eaux*: Presses internationales Polytechnique.

ECO:LOGIC. (2009). NID Regional Water Supply Project -Technical Memorandum Water

Treatment Process Screening. Retrieved from http://nidwater.com/wp-content/uploads/2012/04/Water-Treatment-Process-Screening-May-2009-1-of-2.pdf

Fukuzaki, S., Urano, H., & Nagata, K. (1995). Adsorption of protein onto stainless-steel surfaces. *Journal of Fermentation and Bioengineering, 80*(1), 6-11. doi:http://dx.doi.org/10.1016/0922-338X(95)98168-K

Gregory, J., & Barany, S. (2011). Adsorption and flocculation by polymers and polymer mixtures. *Adv Colloid Interface Sci, 169*(1), 1-12. doi:10.1016/j.cis.2011.06.004

Guezennec, A. G., Michel, C., Bru, K., Touze, S., Desroche, N., Mnif, I., & Motelica-Heino, M. (2015). Transfer and degradation of polyacrylamide-based flocculants in hydrosystems: a review. *Environmental Science and Pollution Research, 22*(9), 6390-6406. doi:10.1007/s11356-014-3556-6

Hodur, C. (2008). Filtration I–Determining Filterability of Suspensions *Experiments in Unit Operations and Processing of Foods* (pp. 21-26): Springer.

Huang, H., Young, T. A., & Jacangelo, J. G. (2008). Unified Membrane Fouling Index for Low Pressure Membrane Filtration of Natural Waters: Principles and Methodology. *Environmental Science & Technology, 42*(3), 714-720. doi:10.1021/es071043j

Jeschke, R., & Hansen, D. (1999). *Water Quality Data From a Full Scale Microsand Ballasted Flocculation and Clarification Plant.* Paper presented at the AWWA Annual Conference, Chicago, IL.

Kawamura, S. (2000). *Integrated design and operation of water treatment facilities* (2nd ed.). New York ; Toronto: John Wiley & Sons.

Kronberg, B., Holmberg, K., & Lindman, B. (2014). *Surface Chemistry of Surfactants and Polymers* Somerset, GB: Wiley.

Lapointe, M., & Barbeau, B. (2016). Characterization of ballasted flocs in water treatment using microscopy. *Water research, 90*, 119-127. doi:http://dx.doi.org/10.1016/j.watres.2015.12.018

Layson, A. (2010). Integrated Ballasted/High Rate Clarification & Membrane Filtration Systems - Design, Operation and Optimisation. Retrieved from http://www.ewisa.co.za/literature/files/326_256%20Layson.pdf

Lee, G. (2000). Upgrading of a Conventional Surface Water Treatment Plant Utilizing Ultra Filtration Membrane Technology Preceded by Ballasted Coagulation Flocculation

ClarificationEnvironmental and Pipeline Engineering 2000 (pp. 317-327). Retrieved from http://ascelibrary.org/doi/abs/10.1061/40507%28282%2936. doi:doi:10.1061/40507(282)36

Lefrançois, P. (2015). *Project: Treatment process Actiflo-UF*. Veolia Water Technologies.

Letterman, R. D., & American Water Works Association. (1999). *Water quality and treatment : a handbook of community water supplies* (5th ed.). New York ; Montreal: McGraw-Hill.

Lin, C.-F., Liu, S.-H., & Hao, O. J. (2001). Effect of functional groups of humic substances on uf performance. *Water research, 35*(10), 2395-2402. doi:http://dx.doi.org/10.1016/S0043-1354(00)00525-X

Loff, L. G. (2001). 8 - Filter media, filter rating. In L. Svarovsky (Ed.), *Solid-Liquid Separation (Fourth Edition)* (pp. 281-301). Oxford: Butterworth-Heinemann.

Lu, J. H., Wu, L., & Letey, J. (2002). Effects of Soil and Water Properties on Anionic Polyacrylamide Sorption. *Soil Science Society of America Journal, 66*(2), 578-584. doi:10.2136/sssaj2002.5780

Ma, Q., Shuler, P. J., Aften, C. W., & Tang, Y. (2015). Theoretical studies of hydrolysis and stability of polyacrylamide polymers. *Polymer Degradation and Stability, 121*, 69-77. doi:http://dx.doi.org/10.1016/j.polymdegradstab.2015.08.012

Majam, S., & Thompson, P. (2006). Polyelectrolyte determination in drinking water. *Water SA, 32*(5).

Ministère du Développement durable, de l'Environnement et de la Lutte contre les changements climatiques (MDDELCC). (2009). Fiche d'évaluation technique du comité sur les technologies de traitement en eau potable ACTIFLO® + DUSENFLO® JOHN MEUNIER INC. . Retrieved from http://www.mddelcc.gouv.qc.ca/eau/potable/guide/actiflo.pdf

Ministère du Développement durable, de l'Environnement et de la Lutte contre les changements climatiques (MDDELCC). (2015a). Guide de conception des installation de production d'eau potable Retrieved from http://www.mddelcc.gouv.qc.ca/eau/potable/guide/index.htm

Ministère du Développement durable, de l'Environnement et de la Lutte contre les changements climatiques (MDDELCC). (2015b). Procédure d'analyse des technologies de traitement en eau potable. Retrieved from http://www.mddelcc.gouv.qc.ca/eau/potable/guide/fiches.htm

Mwangi, I. W., Ngila, J. C., Ndungu, P., & Msagati, T. A. M. (2013). Method Development for the Determination of Diallyldimethylammonium Chloride at Trace Levels by Epoxidation Process. *Water, Air, & Soil Pollution, 224*(9), 1-9. doi:10.1007/s11270-013-1638-6

O'Brien, A. (2006). *First Two Years of Operation: Coagulation and Clarification Ahead of Ultrafiltration for Treating Delta Water in California.* Paper presented at the American Water Works Association - AWWA Annual Conference and Exposition, ACE 2006: The World's Water Event, San Antonio, Texas, USA.

Plum, V., Dahl, C. P., Bentsen, L., Petersen, C. R., Napstjert, L., & Thomsen, N. B. (1998). The Actiflo method. *Water Science and Technology, 37*(1), 269-275. doi:http://dx.doi.org/10.1016/S0273-1223(97)00778-6

Ren, G. M., Sun, D. Z., & Chung, J. S. (2006). Kinetics study on photochemical oxidation of polyacrylamide by ozone combined with hydrogen peroxide and ultraviolet radiation. *J. Environ Sci, 18*(4), 660-664.

Ripperger, S., Gösele, W., Alt, C., & Loewe, T. (2000). Filtration, 1. Fundamentals *Ullmann's Encyclopedia of Industrial Chemistry*: Wiley-VCH Verlag GmbH & Co. KGaA.

Samoshina, Y., Diaz, A., Becker, Y., Nylander, T., & Lindman, B. (2003). Adsorption of cationic, anionic and hydrophobically modified polyacrylamides on silica surfaces. *Colloids and Surfaces A: Physicochemical and Engineering Aspects, 231*(1–3), 195-205. doi:http://dx.doi.org/10.1016/j.colsurfa.2003.09.005

Solberg, D., & Wågberg, L. (2003). Adsorption and flocculation behavior of cationic polyacrylamide and colloidal silica. *Colloids and Surfaces A: Physicochemical and Engineering Aspects, 219*(1–3), 161-172. doi:http://dx.doi.org/10.1016/S0927-7757(03)00029-3

Stuart, B. H. (2005). Spectral Analysis *Infrared Spectroscopy: Fundamentals and Applications* (pp. 45-70): John Wiley & Sons, Ltd.

Sutherland, K. (2008). Section 3 - Types of Filter *Filters and Filtration Handbook (Fifth Edition)* (pp. 97-207). Oxford: Elsevier.

Tchio, M., Koudjonou, B., Desjardins, R., Prévost, M., & Barbeau, B. (2003). A practical guide for determining appropriate chemical dosages for direct filtration. *Canadian Journal of Civil Engineering, 30*(4), 754-757.

Tramfloc, Inc. (2014). Filterability Index. Retrieved from http://tramfloc.com/filterability-index/

United States Environmental Protection Agency (EPA). (2005). *Membrane Filtration Guidance Manual*. Retrieved from http://nepis.epa.gov/Exe/ZyPDF.cgi/901V0500.PDF?Dockey=901V0500.PDF

USEPA. (1999). Alternative Disinfectants and Oxidants Guidance Manual. Retrieved from http://nepis.epa.gov/Exe/ZyPDF.cgi/2000229L.PDF?Dockey=2000229L.PDF

Veolia Water Technologies. (2015). ACTIFLO® The ultimate clarifier. Retrieved from http://www.veoliawatertechnologies.ca/johnmeunier/ressources/files/1/41274,150198_ACTIFLO_Canada_HR.pdf

Ville de Laval. (2003). Les usines de production d'eau potable de Laval. Retrieved from https://www.laval.ca/Documents/Pages/Fr/Citoyens/environnement-recyclage-et-collectes/usines-eau-potable.pdf

Wakeman, R. J., & Tarleton, E. S. (2005). *Solid/liquid separation: Principles of industrial filtration* (Vol. 1st --). Oxford, U.K: Elsevier.

World Health Organization (WHO). (2011). Guidelines for drinking-water quality. Fourth edition. Retrieved from http://www.who.int/water_sanitation_health/publications/2011/dwq_guidelines/en/

Yi, X. S., Shi, W. X., Yu, S. L., Sun, N., Jin, L. M., Wang, S., . . . Sun, L. P. (2012). Comparative study of anion polyacrylamide (APAM) adsorption-related fouling of a PVDF UF membrane and a modified PVDF UF membrane. *Desalination, 286*, 254-262. doi:http://dx.doi.org/10.1016/j.desal.2011.11.032

Yi, X. S., Shi, W. X., Yu, S. L., Wang, Y., Sun, N., Jin, L. M., & Wang, S. (2011). Isotherm and kinetic behavior of adsorption of anion polyacrylamide (APAM) from aqueous solution using two kinds of PVDF UF membranes. *Journal of Hazardous Materials, 189*(1–2), 495-501. doi:http://dx.doi.org/10.1016/j.jhazmat.2011.02.063

Young, J. C., & Edwards, F. G. (2003). Factors affecting ballasted flocculation reactions. *Water environment research*, 263-272.

APPENDIX A – EXPERIMENTAL SETUP OF FILTERABILITY TESTS USING MICROSTRAINERS

Filter holder
13 mm dia.

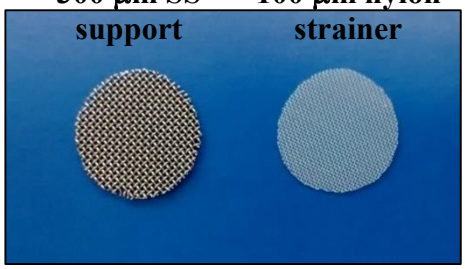

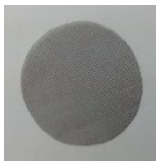

75 µm SS
strainer

103 µm SS
strainer

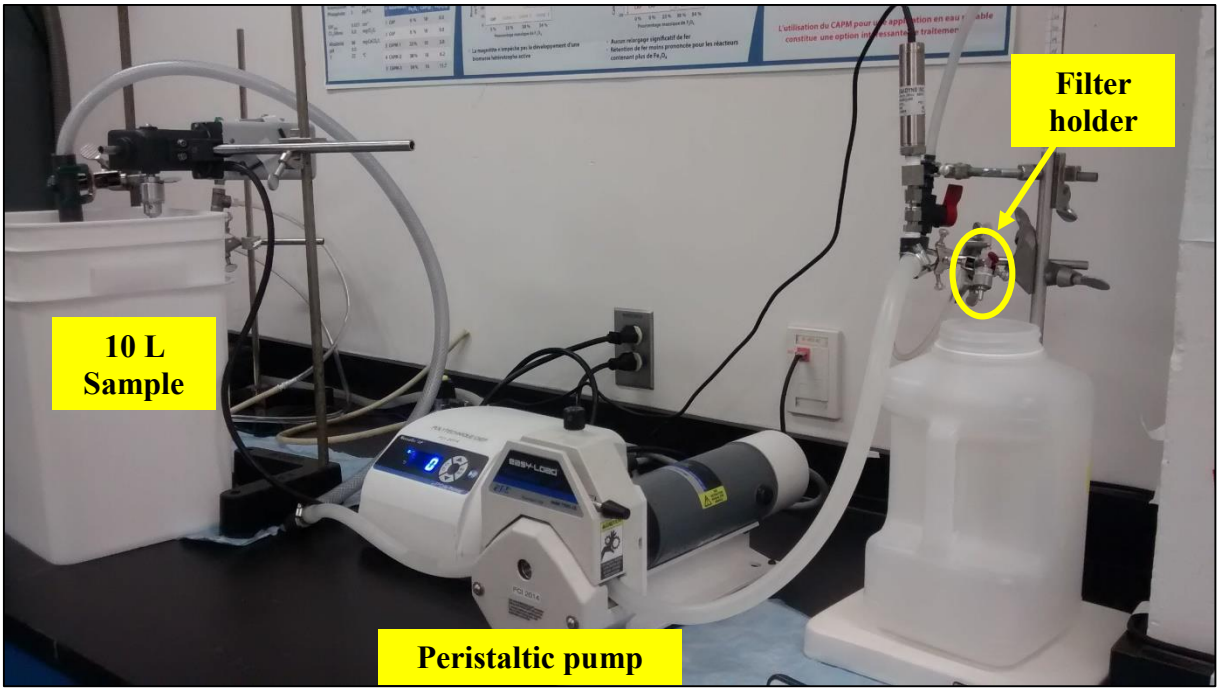

APPENDIX B – OPERATIONAL DATA OF PONT-VIAU ACTIFLO® DURING FILTERABLITY TEST ON SITE

Flow rate: 43443 ± 2016 m^3/d

Upflow velocity: 41 ± 2 m/h

Coagulant dose: 42 ± 5 mg/L dry Alum

Activated silica: 1.25 mg/L (coagulant aid)

Polymer dose: 0.26 mg/L

Microsand effective diameter: 85 μm

Microsand dose: 3.88 ± 1.01 g/m^3

APPENDIX C – CHARACTERIZATION OF FLOCCULATED WATER OF DIFFERENT ACTIFLO®

Parameter	Unit	Pont-Viau	St-Damase	Lévis
		FW	FW	FW
pH		6.82	7.03	7.64
Temperature	°C	22	20	21
Turbidity	NTU	1.2	42	15
Alkalinity	mg $CaCO_3$/L	17	57	70
Conductivity	µS/cm	107	290	283
SCV		-265	-140	-111
UVA_{254nm}	m^{-1}	5.45	N/A	4.30
DOC	mg C/L	3.08	N/A	2.59
$SUVA_{254nm}$	L/mg C · m^{-1}	1.77	N/A	1.66
TOC	mg C/L	N/A	3.97	3.50
TSS	mg/L	11.5	542	178
VSS	mg/L	2.5	7.9	5.6
Particle concentration (>2 µm)	#/mL	3 204	7 489	10 280
Largest particle detected	µm	203.0	306.3	205.5

APPENDIX D – CHARACTERIZATION OF CLARIFIED WATER IN FILTERABILITY TESTS FOR EACH SS STRAINER

Clarified water from Pont-Viau Actiflo®					
Strainer opening size	**Turbidity**	**TSS**	**VSS**	**VSS/TSS**	**Particle concentration (>2 μm)**
μm	**NTU**	**mg/L**	**mg/L**	**%**	**#/mL**
75	0.70 ± 0.10	2.5 ± 0.8	0.77 ± 0.06	33 ± 9	949 ± 56
103	0.69 ± 0.06	2.0 ± 0.4	0.65 ± 0.09	34 ± 5	932 ± 239
152	1.29 ± 0.43	3.8 ± 1.7	1.09 ± 0.47	29 ± 5	2060 ± 302

APPENDIX E – NORMAL PROBABILITY PLOT OF FOULING COEFFICIENTS

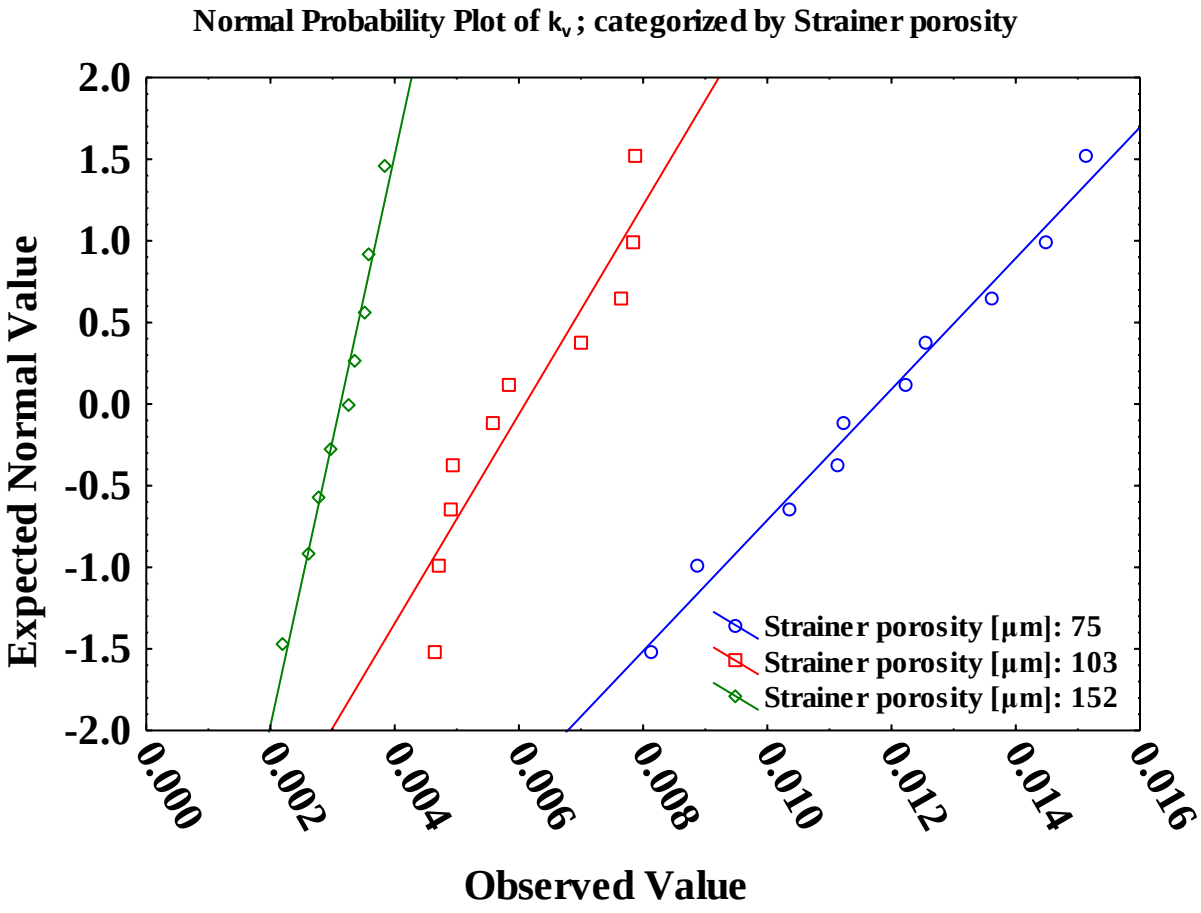

APPENDIX F – FACTORIAL ANOVA UNDER ALKALINE CONDITIONS (PH ≥ 11)

Software: STATISTICA 12

Effect	Univariate Results for Each DV (Statistical analysis_All data in Workbook_All data) Sigma-restricted parameterization Effective hypothesis decomposition				
	Degr. of Freedom	Solids removal [%] SS	Solids removal [%] MS	Solids removal [%] F	Solids removal [%] p
Intercept	1	70427.45	70427.45	931.4983	0.000000
Strainer opening size [µm]	2	988.35	494.18	6.5361	0.020774
BW velocity [m/s]	2	1177.99	589.00	7.7903	0.013248
pH - BW solution	2	20288.73	10144.36	134.1730	0.000001
Strainer opening size [µm]*BW velocity [m/s]	4	386.72	96.68	1.2787	0.354437
Strainer opening size [µm]*pH - BW solution	4	219.80	54.95	0.7268	0.597957
BW velocity [m/s]*pH - BW solution	4	856.46	214.11	2.8319	0.098162
Error	8	604.85	75.61		
Total	26	24522.91			

Interaction effect between backwash velocity and pH

Significant difference (p-values < 0.05) between interactions of each level of each variable

Cell No.	LSD test; variable Solids removal [%] (Statistical analysis_All data in Workbook_All data) Probabilities for Post Hoc Tests Error: Between MS = 75.607, df = 8.0000										
	BW velocity [m/s]	pH - BW solution	(1)	(2)	(3)	(4)	(5)	(6)	(7)	(8)	(9)
1	0.16	5.9		0.084593	0.000008	0.664970	0.019387	0.000008	0.068017	0.000205	0.000008
2	0.16	11.0	0.084593		0.000038	0.167357	0.370556	0.000038	0.891700	0.002141	0.000040
3	0.16	12.6	0.000008	0.000038		0.000011	0.000092	0.989915	0.000043	0.006043	0.954303
4	0.24	5.9	0.664970	0.167357	0.000011		0.038878	0.000011	0.135679	0.000335	0.000011
5	0.24	11.0	0.019387	0.370556	0.000092	0.038878		0.000091	0.442380	0.008070	0.000098
6	0.24	12.6	0.000008	0.000038	0.989915	0.000011	0.000091		0.000043	0.005931	0.944242
7	0.35	5.9	0.068017	0.891700	0.000043	0.135679	0.442380	0.000043		0.002585	0.000046
8	0.35	11.0	0.000205	0.002141	0.006043	0.000335	0.008070	0.005931	0.002585		0.006582
9	0.35	12.6	0.000008	0.000040	0.954303	0.000011	0.000098	0.944242	0.000046	0.006582	

APPENDIX G – MAIN EFFECTS ANOVA OF BACKWASHING FACTORS (UNDER OXIDIZING AND ALKALINE CONDITIONS)

Software: STATISTICA 12

Effect	Univariate Results for Each DV (Statistical analysis_All data in Workbook_All data) Sigma-restricted parameterization Effective hypothesis decomposition				
	Degr. of Freedom	Solids removal [%] SS	Solids removal [%] MS	Solids removal [%] F	Solids removal [%] p
Intercept	1	39571.76	39571.76	403.2416	0.000000
Strainer opening size [µm]	2	1267.15	633.58	6.4562	0.005489
BW velocity [m/s]	2	1213.48	606.74	6.1828	0.006582
pH - BW solution	4	23099.70	5774.92	58.8473	0.000000
Error	25	2453.35	98.13		
Total	33	29435.77			

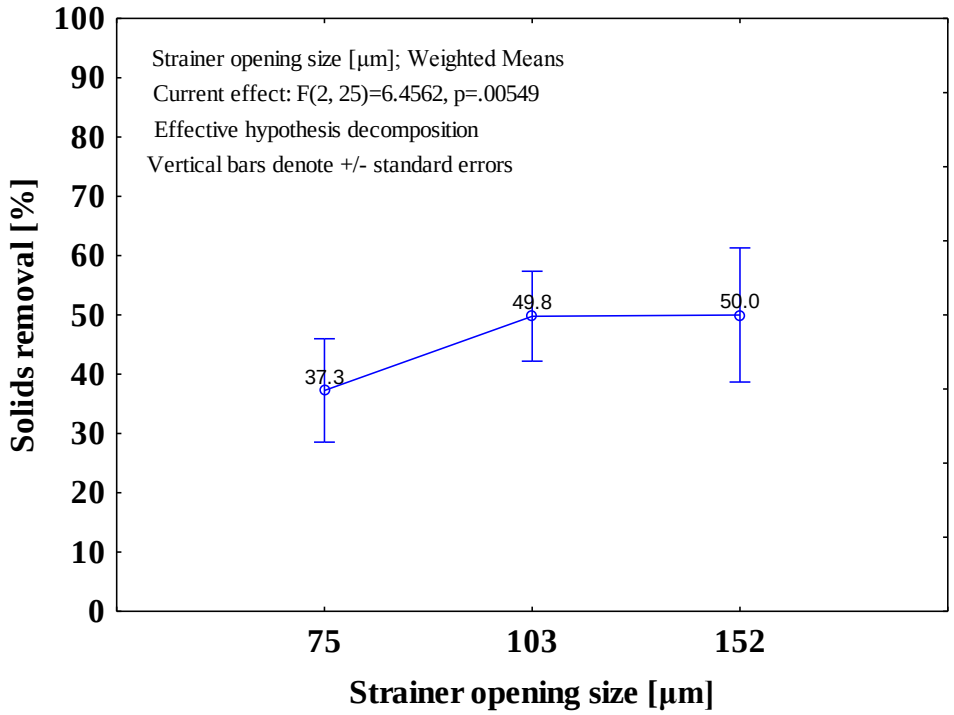

Cell No.	LSD test; variable Solids removal [%] (Statistical analysis_All data in Workbook_All data) Probabilities for Post Hoc Tests Error: Between MS = 98.134, df = 25.000			
	Strainer opening size [µm]	(1) 37.258	(2) 49.776	(3) 49.988
1	75		0.004133	0.007415
2	103	0.004133		0.961050
3	152	0.007415	0.961050	

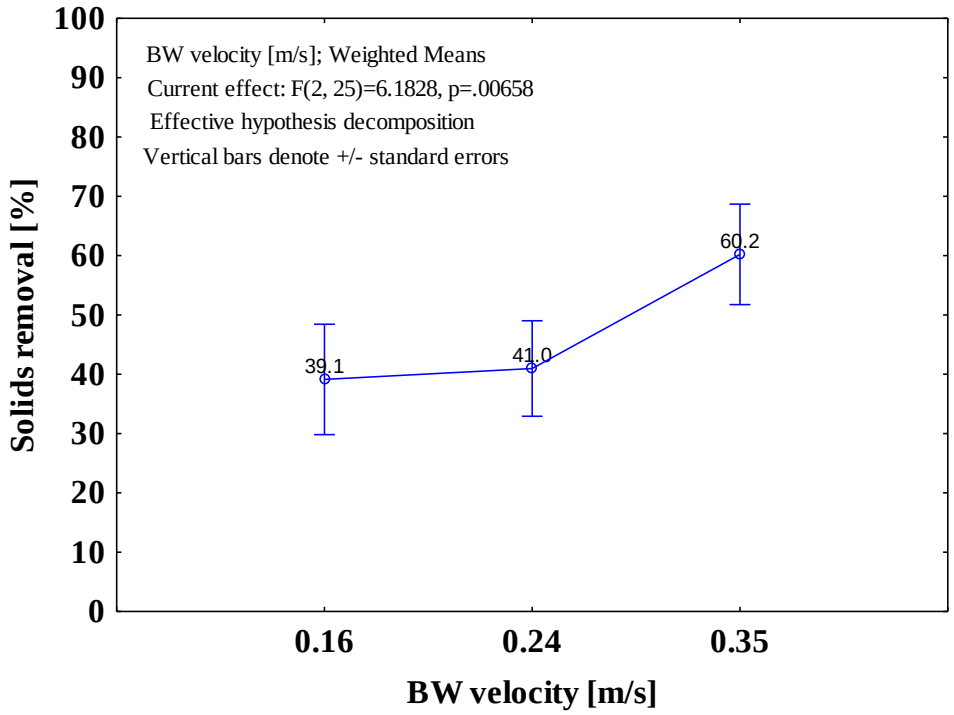

Cell No.	LSD test; variable Solids removal [%] (Statistical analysis_All data in Workbook_All data) Probabilities for Post Hoc Tests Error: Between MS = 98.134, df = 25.000			
	BW velocity [m/s]	(1) 39.129	(2) 40.971	(3) 60.213
1	0.16		0.646447	0.000058
2	0.24	0.646447		0.000144
3	0.35	0.000058	0.000144	

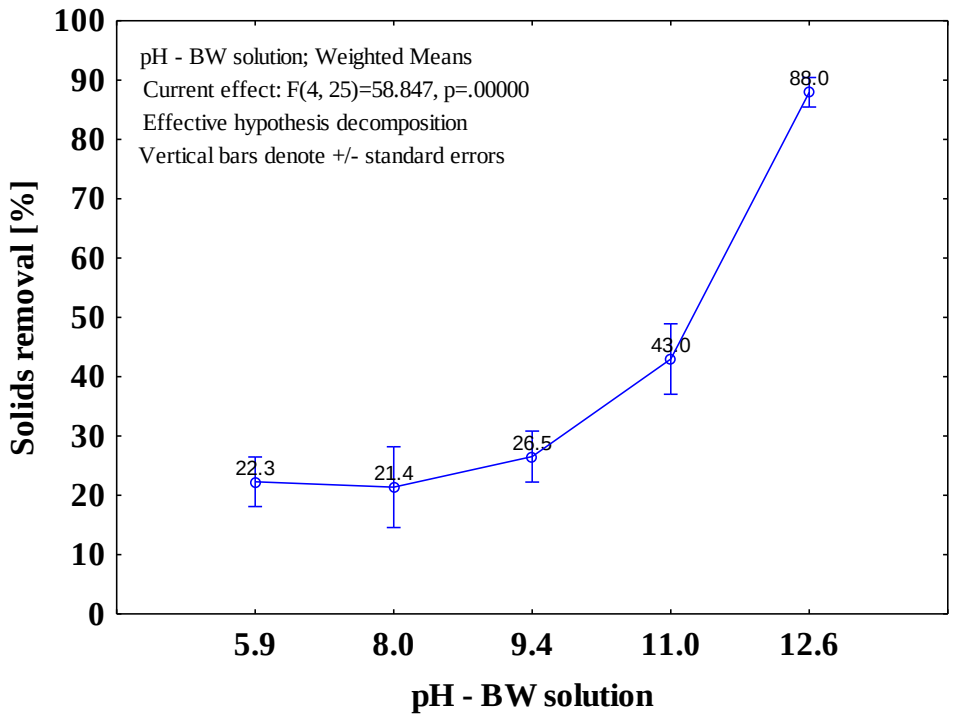

Cell No.	LSD test; variable Solids removal [%] (Statistical analysis_All data in Workbook_All data) Probabilities for Post Hoc Tests Error: Between MS = 98.134, df = 25.000					
	pH - BW solution	(1) 22.286	(2) 21.378	(3) 26.536	(4) 42.979	(5) 87.953
1	5.9		0.879948	0.525701	0.000163	0.000000
2	8.0	0.879948		0.501617	0.001277	0.000000
3	9.4	0.525701	0.501617		0.019791	0.000000
4	11.0	0.000163	0.001277	0.019791		0.000000
5	12.6	0.000000	0.000000	0.000000	0.000000	